



ELSEVIER

Available online at www.sciencedirect.com

LITHOS

Lithos xx (2007) xxx – xxx

www.elsevier.com/locate/lithos

Petrology, geochemistry and paleomagnetism of the earliest magmatic rocks of Deccan Volcanic Province, Kutch, Northwest India

Dalim K. Paul ^{a,*}, Arijit Ray ^a, Brindaban Das ^a, Shiva K. Patil ^b, Sanjib K. Biswas ^a

^a Department of Geology, Presidency College, Calcutta 700073, India

^b Indian Institute of Geomagnetism, Alibagh, Maharashtra, India

Received 23 October 2006; accepted 6 August 2007

Abstract

Tholeiites and alkali basalts occurring in the southern coastal belt of Kutch rift basin, Gujarat are the northernmost on-land exposure of Deccan Traps. Further north, mafic dykes, sill and a differentiated alkaline plutonic complex occur along deep-seated rift-related faults. The major rift-related faults provided the channel ways for the emplacement of the magmas to the surface. These magmatic rocks have been classified into three Groups on the basis of spatial distribution, mode of occurrence and petrochemistry. Petrological, geochemical and paleomagnetic data for the representative samples of the volcanic and intrusive rocks from Kutch region are presented. The alkali basalts are enriched in LILE and LREE compared to the Deccan tholeiitic basalts. Paleomagnetic investigations of thirty magmatic bodies of Kutch yield a Virtual Geomagnetic Pole (VGP) at 33.7°N and 81.2°W (dp/dm=5.81/9.18). This obtained pole is statistically concordant with that of the Deccan Super Pole (36.9°N:78.7°W). The magmatic rocks of the Kutch basin are broadly contemporaneous straddling 30N–29R–29N chrons. It is suggested that the magmatic rocks of Kutch were generated by the impact of the Réunion plume on the Kutch lithosphere under extensional setting.

© 2007 Published by Elsevier B.V.

Keywords: Deccan Volcanic Province; Paleomagnetism; Petrogenesis; Plume; Rift

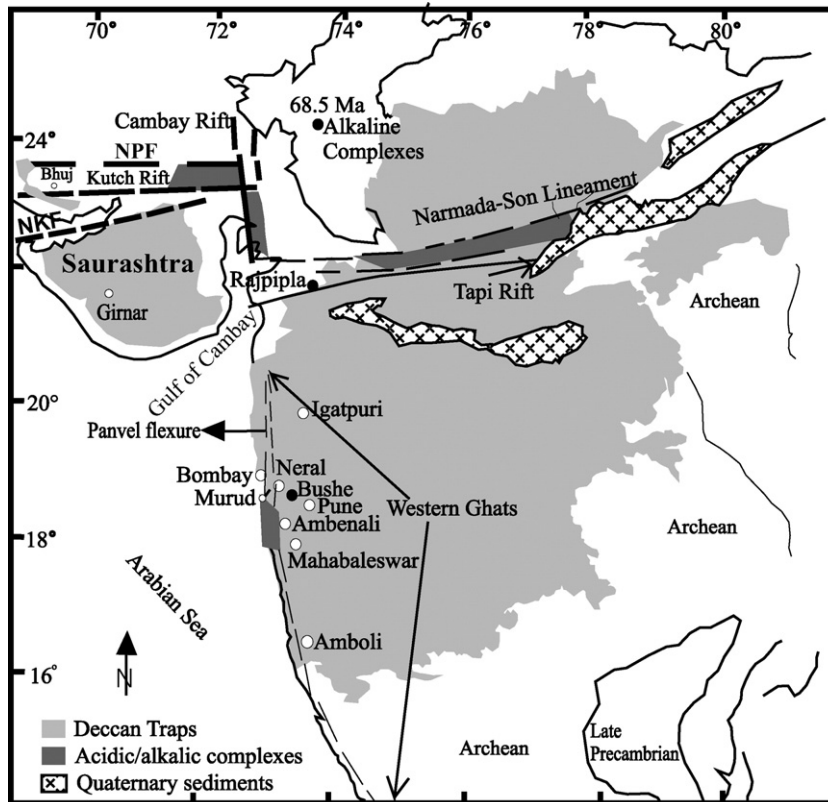
1. Introduction

The Deccan Traps cover an area of about 500,000 sq. km in Western India (Fig. 1). Considerable thickness of Deccan Trap flows also extends over the continental shelf almost up to the 68° E longitude. To the north, the flows extend up to the southern part of Kutch District of Gujarat across the Gulf of Kutch. The magmatic rocks of Kutch mark the northern limit of the Deccan Trap volcanic activities that took place during Late Creta-

ceous–Early Paleocene period across the K–T bound-
ary (Shukla et al., 2001), when the Indian plate passed
over the Réunion hot spot. Some of the oldest flows of
the Deccan volcanic activity are exposed along the
coastal belt of the Gulf of Kutch. Further north, the
Deccan Traps thin out against the Mesozoic rocks and
were eroded away barring a few outliers. The erosion of
the Trap cover exposed several feeder plugs and other
intrusives and a few volcanic vents. Besides, the petro-
chemical comparison of the Deccan Traps of north-
western India (including Kutch region) and the well-
studied sections of the Western Ghats make the rocks of
Kutch particularly interesting to study.

* Corresponding author.

E-mail address: dalimpaul@yahoo.co.in (D.K. Paul).



NPF - Nagar Parkar Fault
NKF - North Kathiawar Fault

Fig. 1. Map of western India showing the location of the Deccan Volcanic Province (DVP) (light shaded area), the Son-Narmada lineament, the Cambay and Kutch rifts. Distribution of alkaline complexes in the DVP is also shown (dark shaded area). Location of Bhuj, area of the present study, is in the western corner.

46 1.1. Geological setting

47 1.1.1. Tectonic framework and structure

48 The Kutch Basin located at the western margin of the
49 Indian craton, is an east-west oriented pericratonic rift-
50 basin (Biswas, 2002). The Nagar Parkar Fault (NPF)
51 bounds the rift on the north and the North Kathiawar
52 Fault (NKF) limits it to the south (Fig. 2a). The rift basin
53 is featured by intra-basin tilted fault blocks and inter-
54 vening half-grabens (Fig. 2b). The uplifts stand out
55 conspicuously as highlands amidst the extensive mud
56 and salt flat over the intervening structural lows-Rann
57 Graben (RG), Banni Half-Graben (BHG) and Gulf of
58 Kutch Half-Graben (GOK). Rocks are exposed in the
59 highlands whereas the flatlands are covered by Holo-
60 cene sediments. Three uplifts occur along parallel strike
61 faults forming ridges of varying dimensions. These east-
62 west trending uplifts are (Fig. 2a): the Island Belt Uplift
63 (IBU) to the north, the Kutch Mainland Uplift (KMU)
64 in the south with the Wagad Uplift (WU) in the central

part. The “Island Belt” is a metaphorical name given to
65 an E–W chain of highlands standing like “islands” on
66 the vast expanse of the mud and salt flat. The Island Belt
67 Uplift along the E–W master fault consists of four
68 smaller uplifts separated by NE–SW wrench faults, viz.,
69 Pachham Uplift (PU), Khadir Uplift (KU), Bela Uplift
70 (BU) and Chorar Uplift (CU) (Fig. 2a) forming a chain
71 of “islands”. The highland representing the largest uplift
72 and the southern segment of the rift basin adjacent to the
73 Gulf of Kutch is known as the “Kutch Mainland”.
74

A first order meridional basement high called Median
75 High (MH) extends across the uplifts and the half-
76 grabens (Fig. 2a). This High divides the Kutch Mainland
77 Uplift symmetrically and the Pachham Uplift is situated
78 on it. On the east, the rift basin terminates against the
79 NW–SE trending Radhanpur–Barmer basement Arch
80 that separates this E–W rift and the NW–SE Cambay
81 rift (Fig. 1).
82

The rifting of the Kutch basin started during the early
83 phase of India–Africa separation in Late Triassic–Early
84

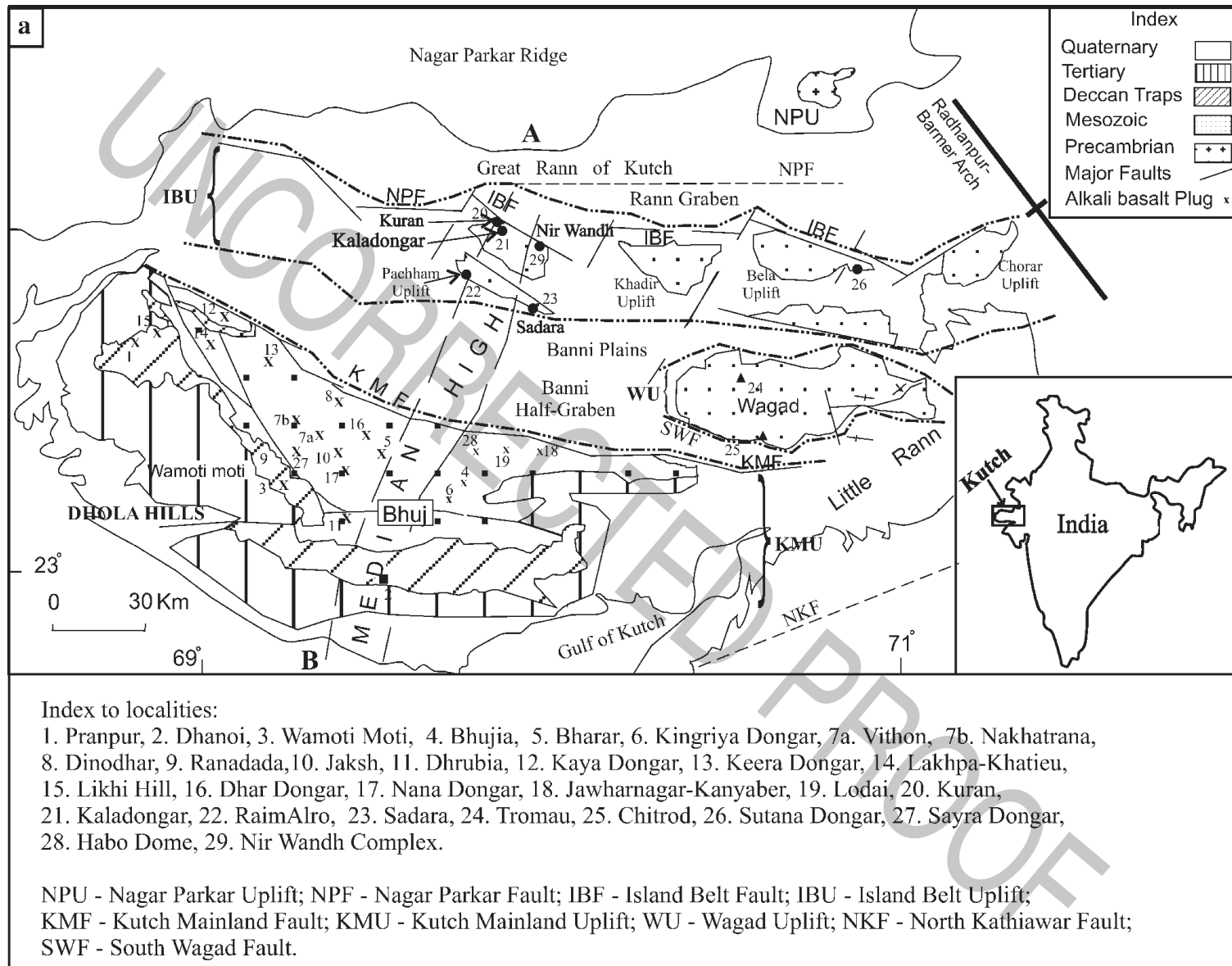


Fig. 2. a: Generalised geological map of Kutch (after Biswas, 2002) showing sampling sites for the present study. For abbreviations see text under Geologic setting-tectonic framework. b: Geological section along AB in Fig. 2a. The intrusives in the northern Island Belt Uplift occur along the deep faults shown in the section.

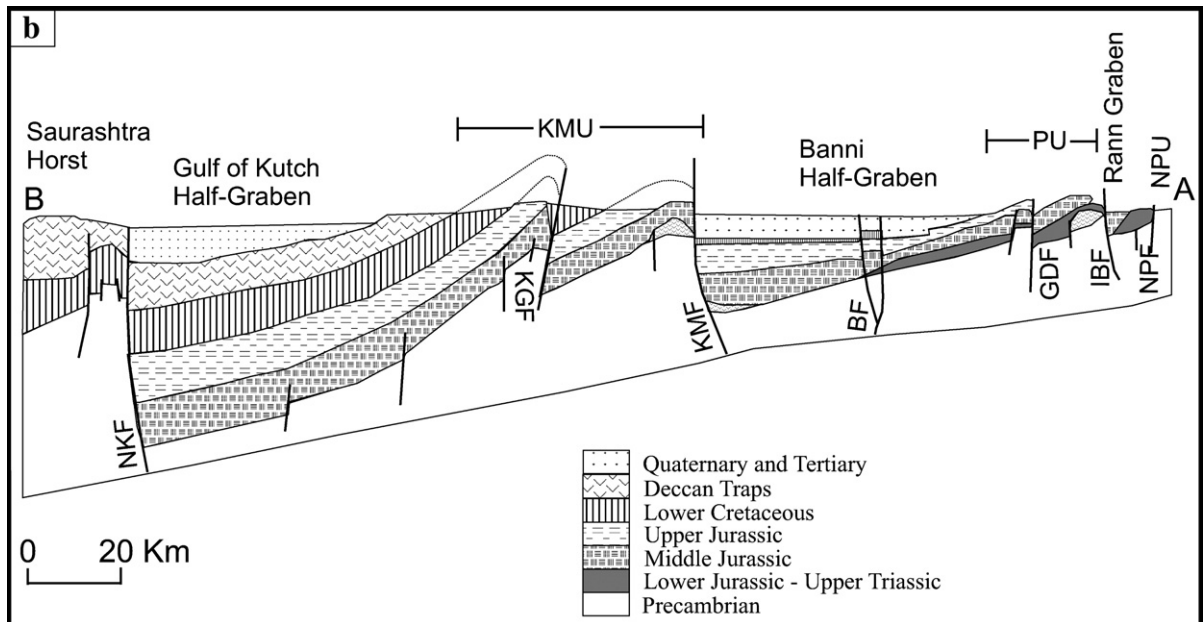


Fig. 2 (continued).

85 Jurassic and ended with the rift-drift transition of the
 86 Indian plate in Early Cretaceous as the Seychelles–
 87 Mascarene Plateau finally rifted away from Western
 88 India (Biswas, 1987).

89 1.1.2. Magmatic activity

90 The Mesozoic rocks of the Kutch Basin were affected
 91 by intense magmatic activities that left signatures in the
 92 form of dykes, sills, plugs, laccoliths and ring dykes.
 93 These magmatic rocks can be classified into three
 94 groups, on considerations of spatial distribution and
 95 mode of occurrence in relation to tectonic setting: tho-
 96 leiitic basalt, dolerite and gabbroic dykes of Kutch
 97 Mainland; alkali basalt plugs of Kutch Mainland; and
 98 the alkaline intrusives including lamprophyres of Kutch
 99 Island Belt. The eruptive activity is represented by alkali
 100 basalt and tholeiitic basalt flows (Guha et al., 2005).
 101 Magmatic rocks are fairly common in all the uplift areas.
 102 Gravity-magnetic data indicate the presence of igneous
 103 intrusives beneath the recent sediment cover in the
 104 structural lows (Biswas, 1980). They are mainly con-
 105 centrated in the narrow deformation zones accompa-
 106 ny the master faults of the uplifts. The maximum
 107 density of magmatic activity is present in the north-
 108 western part of Kutch Mainland Uplift, west of the
 109 Median High and in the northern part of Pachham
 110 Uplift. The occurrence of dykes and other intrusives
 111 along faults and in the marginal deformation zones of
 112 the uplifts indicate the control of the pre-existing tec-
 113 tonic elements of the basin in the emplacement of the

magmatic rocks. A number of alkali basalt plugs occur 114
 along a belt in the central region of Kutch Mainland and 115
 several alkaline intrusives occur in the northern part of 116
 Pachham Island (Fig. 2a). In other uplifts in eastern 117
 Kutch, only dykes and sills are present. In the domi- 118
 nantly tholeiitic Deccan Volcanic Province, alkaline 119
 rocks are volumetrically small (Bose, 1980). Alkaline 120
 rocks are, however, known in the neighboring areas of 121
 Gujarat and Maharashtra from Mount Girnar Igneous 122
 Complex (Bose, 1973; Paul et al., 1977), Amba Dongar 123
 Carbonatite Complex (Chatterjee et al., 1992), Rajpipla 124
 (Mahoney, 1988) and around Murud, south of Mumbai 125
 (Dessai et al., 1990) (Fig. 1). Of all these, only the 126
 alkaline basalts of Kutch contain ultramafic (mostly 127
 wehrlite) xenoliths. 128

Tholeiitic basalt flows are exposed only in the southern 129
 part of Kutch Mainland in a 10 km wide belt forming the 130
 Dhola Hills (Fig. 2a). The Deccan Traps continue beneath 131
 the Tertiary sediments towards south in the Gulf of 132
 Kutch and across the North Kathiawar Fault (Fig. 2a). It is 133
 exposed again in Saurashtra plateau (Biswas and 134
 Deshpande, 1973). In the adjacent Cambay rift and 135
 further south in the western offshore basin, the Deccan 136
 Traps form the basement of Tertiary sediments. Thus, the 137
 tholeiitic basalts of Kutch are continuous with the Deccan 138
 Volcanic Province of western India. The progressive 139
 northward thinning of the Deccan Traps from 1500 m in 140
 the Deccan Volcanic Province type area in Maharashtra to 141
 100 m in Kutch and breaking up of outcrops into detached 142
 outliers farther north suggests that the Kutch and North 143

Gujarat outcrops are the northernmost occurrences of the Deccan Traps. The Kutch Mainland Fault marks the northern limit of the volcanic field. This is corroborated by the absence of tholeiitic basalt flows further north beyond the Kutch Mainland Fault and in the intervening structural lows as indicated by the geophysical as well as deep drilling data (source-Oil & Natural Gas Corporation Ltd., India). The tholeiitic basalt flows disconformably overlie the Mesozoic rocks.

In this paper, we present petrological, geochemical and paleomagnetic data on the magmatic rocks of Kutch with a view to explore the relationships among the three groups of magmatic rocks mentioned earlier. Particularly, we want to study the magmatic manifestation of the impact of a mantle plume on the lithosphere beneath the Kutch rift zone and the nature of the subcrustal lithosphere of the region. As the tholeiitic basalts of Kutch are believed to be the oldest flows of the Deccan Volcanic Province (Basu et al., 1993), this area provides an excellent opportunity to study the onset of Deccan volcanism.

2. Petrology and mineralogy

As stated earlier, the magmatic rocks of Kutch basin include both extrusive and intrusive components. The extrusive components are represented by thick flows of tholeiites occurring along the coastal belt of Kutch Mainland Uplift (KMU). Six flows have been traced in the field with a very gentle 5° southerly dip. In close spatial association with the tholeiitic basalts, dolerite and gabbroic intrusives are common in KMU. The intrusive rocks occur in the form of dyke swarm, laccolith and plutons. They are mineralogically similar to the tholeiitic basalts (Table 1). These two categories of magmatic rocks, i.e. the Kutch Mainland tholeiitic basalts, dolerite and gabbro constitute Group-I for the purpose of this paper. A characteristic feature is the occurrence of a large number of alkali basalt plugs in KMU along a linear WNW–ESE belt (Fig. 2a). Most of these plugs are intrusive into the Cretaceous Bhuj Formation and contain mantle derived ultramafic xenoliths (De, 1964; Mukherjee and Biswas, 1988; Krishnamurthy et al., 1989). Some of these alkali basalt plugs are associated with pyroclastics as in Vithon and Dhruvia (Fig. 2a). The ultramafic xenoliths are very small in size (3 cm), mostly platy in character. Compositionally, a majority of the xenoliths are wehrlite with subordinate lherzolite and dunite. These xenolith bearing alkali basalts are not found elsewhere in the Deccan Volcanic Province. The alkali basalts from KMU constitute Group-II magmatic rocks.

In the northern Island Belt Uplift, intrusive rocks occur in the form of dykes, sills and plutons particularly in the Pachham area. Of these, melagabbroic rocks occur around Kuran, mafic dykes at the core of the Kaladongar anticline, mafic sill around Sadara (Ray et al., 2006) and a differentiated plutonic igneous complex around Nir Wandh (Fig. 3). The main rock types in the Nir Wandh include pyroxenite, alkali gabbro, alkali diorite, nepheline syenite and lamprophyre. All these intrusives occur in the zone of intense deformation characterised by faulting and folding (see N–S geological section in Fig. 2b). These intrusive rocks of Pachham Island have been classified under Group-III.

The volcanic rocks of Kutch basin are classified using TAS diagram and the plutonic rocks are classified on the basis of modal mineralogy using QAPF diagram and pyroxene–plagioclase–hornblende diagram of IUGS (Le Bas and Streckeisen, 1991). Petrographic descriptions of these magmatic rocks are given in Table 1.

3. Geochemistry

Major element analyses were carried out using X-ray fluorescence technique with a Philips MagiX-PRO PW2440 fully automatic, microprocessor controlled X-ray spectrometer equipped with a 4 KW X-ray generator. International rock standards from the US Geological Survey and Geological Survey of Japan were used to prepare calibration curves. Total iron was measured as Fe₂O₃, which was converted to FeO and divided between FeO and Fe₂O₃. 85% of the total iron was allotted as FeO and the remaining 15% as Fe₂O₃. The trace elements were determined using a Perkin Elmer SCIEX, Model 6100 ELAN DRC II ICP-Mass Spectrometer with a Meinhard nebulizer for sample introduction. The detailed analytical procedure is given by Balaram and Gnaneshwar Rao (2003). The major and trace element analyses were carried out at the National Geophysical Research Institute laboratories, Hyderabad. The major and trace element composition of International Standard, JB-2, were determined, in duplicate, during the present analysis and the results are given in Table 2. The results indicate the accuracy and precision of the present analytical data.

Major and trace element abundances of representative samples of the magmatic rocks from both the Kutch Mainland and the Island Belt are presented in Table 2. The analytical results on the individual samples are available with the supplementary database of the Journal. The relevant data are plotted in total alkali–silica (TAS) diagram (Le Bas and Streckeisen, 1991) (Fig. 4). In this diagram, the Kuran gabbro samples of the Island Belt plot in the picro-basalt field. The Sadara

t1.1 Table 1

t1.2 Petrographic description of magmatic rocks of Kutch basin

t1.3	Group	Rock type (locality)	Petrographic description	Classification after IUGS (Le Bas and Streckisen, 1992)
t1.4	I	Tholeiite (Pranpur, Dhanoi–Dahisara, Likhi Hill, Wamoti Moti, Fig. 2a)	Porphyritic with microphenocrysts of plagioclase (An ₆₀) set in a groundmass made up of plagioclase, clinopyroxene, ilmenite and glass	Tholeiitic basalt
t1.5	I	Dolerite dyke (Lakhpa–Khatieu, Keera Dongar, Dinodhar, Ranadada, Fig. 2a)	Porphyritic varieties have phenocrysts of plagioclase (An _{60–65}) set in a groundmass composed of clinopyroxene (augite), ilmenite. Medium grained nonporphyritic varieties have plagioclase (An _{50–60}), augite, ilmenite and show sub-ophitic and intergranular texture	Dolerite
t1.6	I	Gabbroic pluton and laccolith (Manjal Dome, Dhar Dongar, Kaya Dongar, Fig. 2a)	Coarse-grained, hypidiomorphic, almost equigranular with plagioclase (An _{64–70}) and augite. Ilmenite is a common accessory mineral with occasional magnetite	Gabbro
t1.7	II	Alkali basalt plug (Dinodhar, Vithon, Dhruvia, Bhujia, Sayara, Nakhatrana, Keera Dongar, Fig. 2a)	Strongly porphyritic with phenocrysts of olivine (Fo _{70–75}). Olivine also occurs as xenocrysts (Fo _{88–90}). Titanaugite occasionally occurs as microphenocrysts but is a common mineral in groundmass. Plagioclase (An ₃₅) occurs as subhedral laths in groundmass along with olivine, clinopyroxene, nepheline, opaque and glass	Alkali olivine basalt (from normative mineralogy); Alkali basalt–basanite using TAS diagram
t1.8	III	Mafic sill of Sadara	Strongly porphyritic with phenocrysts of olivine (Fo _{76–88}). Clinopyroxene (Wo ₅₀ En ₃₆ Fs ₁₄), plagioclase (An _{80–82}). Phenocryst assemblage constitutes about 60% of the rock. Groundmass (0.1–0.3 mm) contains olivine, clinopyroxene, plagioclase and opaque. Porphyritic and glomeroporphyritic texture common, the groundmass is characterized by intergranular and sub-ophitic texture	Porphyritic dolerite/dolerite porphyry
t1.9	III	Mafic dykes of Kaladongar	Porphyritic with phenocrysts of titanaugite and kaersutite set in a groundmass composed of titanaugite, plagioclase, kaersutite, nepheline, biotite and ilmenite	Foid bearing dolerite (theralite)
t1.10	III	Mafic pluton of Kuran	Coarse-grained with occasional phenocrysts of titanaugite set in a groundmass made up of plagioclase (An ₆₀), kaersutite, olivine and minor nepheline	Foid bearing gabbro (theralite)
t1.11	III	Pyroxenite of Nir Wandh	Coarse-grained showing hypidiomorphic and cumulus texture with titanaugite (85–90%), kaersutite, minor plagioclase	Kaersutite bearing pyroxenite
t1.12	III	Gabbroid rocks of Nir Wandh	Coarse-grained, equigranular rock, mesocratic to melanocratic in appearance and composed of titanaugite, zoned plagioclase (An _{55–An₇₅}), kaersutite, alkali feldspar, nepheline and accessory apatite, calcite	Foid monzo gabbro (theralite)
t1.13	III	Dioritic rocks of Nir Wandh	Medium to coarse-grained rock, leucocratic to mesocratic, composed of plagioclase (An _{38–46}), kaersutite, titanaugite, nepheline minor biotite, and alkali feldspar	Foid monzo diorite
t1.14	III	Syenite of Nir Wandh	Coarse-grained, leucocratic rocks with alkali feldspar, nepheline, plagioclase, kaersutite, aegirine augite and accessory calcite, apatite	Nepheline syenite

t1.15 Table 1 (continued)

t1.16 Group	Rock type (locality)	Petrographic description	Classification after IUGS (Le Bas and Streckisen, 1992)
t1.17 III	Lamprophyre dyke of Nir Wandh	Strongly porphyritic with megacrysts of kaersutite, titanite, olivine set in a groundmass composed of kaersutite, titanite, plagioclase alkali feldspar, nepheline, calcite, apatite	Camptonite
t1.18 III	Fine grained mafic dyke of Nir Wandh	Fine-grained mesocratic with plagioclase (An ₆₄), titanite, kaersutite, alkali feldspar and analcime	Microgabbro (Teschentite)

244 sill samples also fall in the basalt field but close to the
 245 basalt–basanite boundary (Ray et al., 2006). These
 246 samples have a close similarity with total alkali varying
 247 from 3.5 to 4.5 wt.%. The Sadara sill is silica under-
 248 saturated (SiO₂: 45–47 wt.%) with MgO varying from
 249 9.2 to 10.7 wt.%. Mg# is variable between 64 and 68.
 250 TiO₂ is around 2 wt.% but the CaO and total iron
 251 contents are higher compared to the continental flood
 252 basalts (Wilson, 1989).

253 The rock types of the Nir Wandh complex have a wide
 254 variation of alkali (1.47 to 11.48 wt.%). As a result, most
 255 of the samples fall in the basalt field but a few plots in the

field of picro-basalt, basaltic andesite, basaltic trachy-
 256 andesite, phono-tephrite and tephri-phonolite. The
 257 tholeiitic basalts and the dykes of Kutch Mainland fall
 258 in the fields of basalt and basaltic andesite. Among the
 259 different rock types studied here, the number of alkali
 260 basalts analysed (36) are comparatively large. These
 261 samples can be classified as tephrite-basanite with a few
 262 as transitional between basalt and tephrite-basanite.
 263

In bivariate plots for the Island Belt rocks (Fig. 5a–f),
 264 CaO and Ni show a positive correlation with MgO,
 265 but K₂O, Al₂O₃ and ΣREE show negative correlation.
 266 (La/Yb)_n has a positive correlation with ΣREE. These
 267

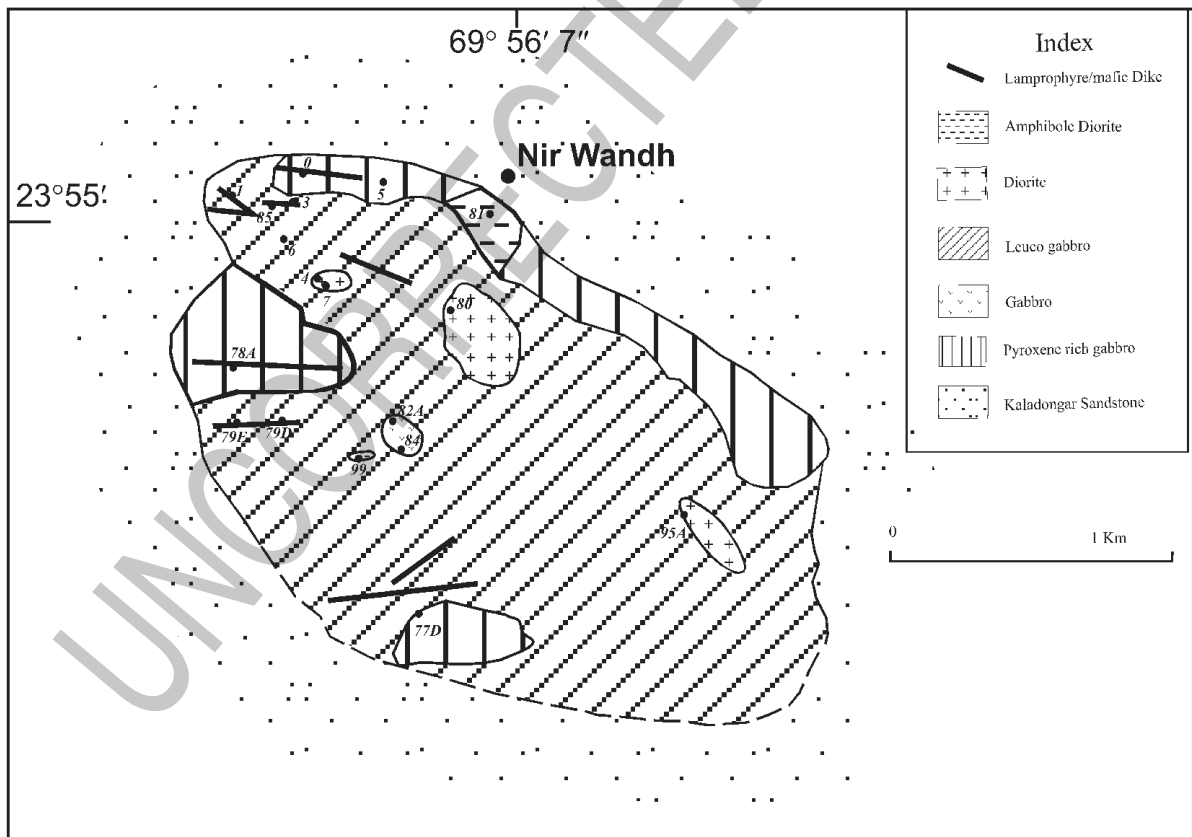
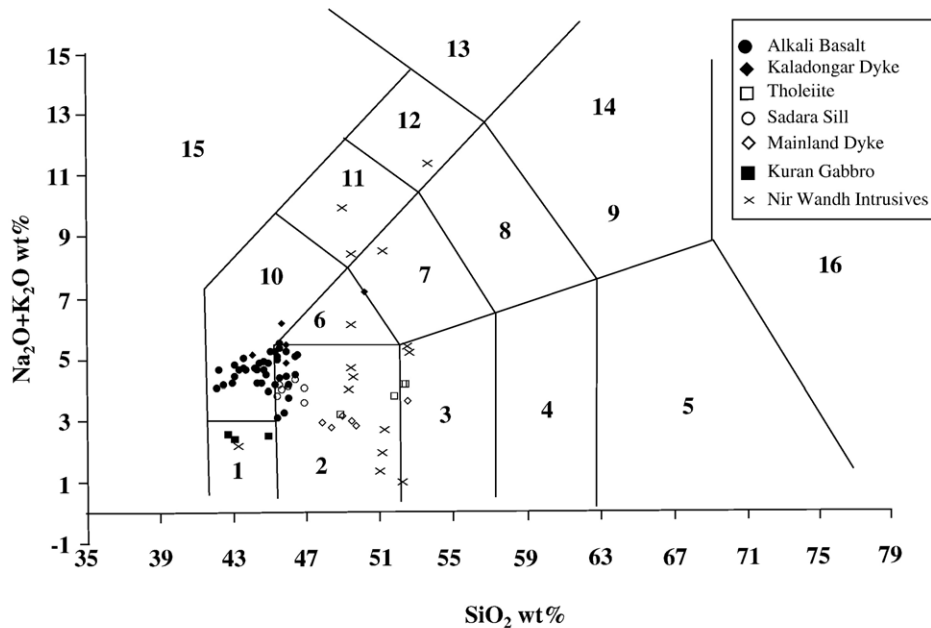


Fig. 3. Geological map of the Nir Wandh Igneous Complex, Island belt, Kutch.

Table 2
Major (wt.%) and trace element (ppm) abundances of representative samples of magmatic rocks, Kutch

Locality	Kala Dongar		Nir Wandh				Nana Dongar	Vithon	Dinodhar	Wamoti Moti	Lodai	Kingriya Dongar	Pranpur	RANADADA	LAKHPA		
Sample	BH32.1	BH33.1	NW-7	NW-85	NW-77A	NW-82A	BH1.1	BH41	BH14.4	BH18.1	LD1.1	BH12.4	BH3.1	BH17.1	BH5.2	JB2	JB2
Rock type	Basalt		Diorite	Pyroxenite	Lamprophyre	Gabbro	Alkali basalt					Tholeiite	Gabbro			Measured	Govindaraju (1994)
SiO ₂	43.94	45.54	51.10	42.84	52.48	50.94	42.93	43.47	42.34	44.69	42.07	44.64	51.66	49.57	48.21	52.98	53.20
TiO ₂	3.20	2.94	1.05	3.56	2.10	1.64	2.15	2.94	3.21	2.68	3.11	3.01	1.55	0.86	2.41	1.17	1.19
Al ₂ O ₃	12.84	14.18	18.81	11.01	13.43	18.99	11.97	11.80	11.06	10.85	11.69	9.04	13.11	15.28	12.93	14.48	14.67
Fe ₂ O ₃	13.55	13.95	8.53	12.6	11.21	8.78	12.76	14.20	13.68	12.99	12.47	12.51	16.57	12.68	14.43	14.24	14.34
MnO	0.17	0.17	0.17	0.14	0.16	0.08	0.17	0.18	0.16	0.17	0.15	0.15	0.19	0.18	0.18	0.19	0.20
MgO	6.47	6.26	4.33	11.96	4.31	3.15	11.89	10.26	10.21	12.75	11.25	9.11	4.35	6.29	7.83	4.48	4.66
CaO	11.85	8.39	5.50	14.26	6.33	13.50	10.34	10.63	10.89	10.19	9.74	13.72	7.73	12.33	9.22	9.72	9.89
Na ₂ O	3.29	4.04	6.67	1.36	4.17	1.29	2.89	3.24	2.92	3.32	2.25	2.44	2.97	1.97	2.04	1.99	2.03
K ₂ O	1.79	2.04	1.97	0.46	1.35	0.18	0.93	1.38	2.98	1.10	2.08	0.87	0.77	0.30	0.67	0.39	0.42
P ₂ O ₅	0.97	1.01	0.49	0.17	0.73	0.05	0.68	0.67	0.47	0.46	0.88	0.98	0.21	0.09	0.33	0.09	0.10
Total	98.07	98.52	98.62	98.36	96.27	98.60	96.71	98.77	97.92	99.20	95.69	96.47	99.11	99.55	98.25	99.73	100.70
Mg#	49	51	54	69	47	46	68	63	64	70	68	63	38	54	56		
Na ₂ O/K ₂ O	1.84	1.98	3.39	2.96	3.09	7.17	3.11	2.35	0.98	3.02	1.08	2.80	3.86	6.57	3.04		
Ba	1820	1675	0.19	205.10	0.20	208.90	564.80	466.30	488.60	448.80	3127.00	1371.00	315.20	114.70	157.80	211.30	208.00
Rb	39.06	51.19	85.41	8.00	50.28	6.62	27.15	37.23	53.34	29.35	77.02	67.70	24.54	10.44	14.90	5.99	6.20
Sr	1416	1220	0.64	393.30	0.30	0.89	603.60	981.20	617.20	593.00	1545.00	1942.00	211.40	131.10	192.60	172.40	178.00
Y	31.79	31.17	40.76	17.20	24.61	10.99	22.15	32.48	24.57	20.98	23.23	28.36	41.98	24.45	34.44	24.66	24.00
Zr	288.40	347.50	398.40	137.20	306.50	82.00	189.00	292.80	234.00	224.40	284.60	352.70	164.30	77.60	172.00	51.10	51.40
Nb	101.95	102.56	135.81	26.80	12.64	11.13	63.23	66.40	55.98	59.78	95.34	149.56	20.21	5.92	16.29	0.79	0.80
Th	8.14	10.53	11.45	1.04	7.22	1.24	6.74	6.90	4.28	5.26	9.75	12.33	4.20	1.70	1.95	0.34	0.33
Pb	23.00	7.78	8.24	7.90	4.53	2.74	18.18	9.98	21.94	22.64	7.49	19.83	19.70	18.04	22.63	5.49	5.40
Ga	34.19	33.59	48.35	15.20	43.52	24.31	19.17	25.03	21.80	20.35	46.80	16.79	20.06	17.03	21.80	17.19	17.00
Zn	194.70	222.50	66.60	130.70	195.40	101.70	189.60	192.60	239.90	199.10	220.10	250.60	153.80	102.40	186.20	116.20	110.00

Cu	120.80	80.74	1.03	57.70	48.50	49.50	102.00	79.30	89.30	95.10	72.90	79.20	223.20	148.50	239.20	231.70	227.00
Ni	48.70	54.70	16.70	82.30	50.20	47.90	260.50	209.50	171.30	447.90	317.70	304.40	28.10	88.60	153.30	14.90	14.20
V	358.50	268.20	5.80	532.10	217.10	389.00	306.90	295.10	329.50	277.90	232.10	205.10	399.10	302.80	377.60	586.60	578.00
Cr	27.23	53.70	0.85	56.00	73.10	11.45	525.51	388.79	330.63	635.10	326.26	296.96	12.69	217.18	90.69	26.32	27.40
Hf	5.82	6.84	6.85	3.90	4.84	2.31	4.09	6.49	5.25	4.52	5.99	6.75	3.69	1.66	3.90	1.47	1.42
Cs	3.13	3.01	1.44	0.10	4.32	0.09	0.63	0.70	0.70	0.63	0.97	0.95	0.71	0.46	0.20	0.90	0.90
Sc	18.66	16.83	1.82	37.10	12.77	16.80	27.00	29.60	25.50	25.00	19.40	20.70	43.80	44.90	35.50	52.60	54.40
Ta	14.90	13.10	7.60	4.30	0.17	1.73	4.16	8.83	3.95	5.91	11.24	12.09	2.12	1.22	1.70	0.21	0.20
Co	58.40	52.30	35.70	70.90	37.60	62.10	78.20	73.50	69.50	89.80	73.30	73.30	63.70	67.00	72.70	41.50	39.80
U	2.02	1.98	3.66	0.00	1.07	0.26	0.78	1.39	0.61	0.83	1.79	1.71	0.53	0.28	0.31	0.17	0.16
La	62.70	67.55	82.31	13.60	66.26	13.09	41.68	46.79	30.50	33.90	57.84	80.54	19.40	6.60	13.18	2.40	2.37
Ce	125.39	131.27	146.05	34.60	115.64	24.54	79.21	97.16	66.26	71.57	106.63	151.49	40.00	14.53	32.42	6.19	6.77
Pr	12.07	12.23	14.44	4.10	13.74	2.77	7.57	9.77	6.95	7.10	10.02	14.06	4.01	1.57	3.68	0.98	0.96
Nd	60.14	60.04	53.18	24.50	48.94	14.05	39.32	51.65	38.03	39.36	49.83	74.44	21.43	9.38	22.99	6.77	6.70
Sm	10.79	10.25	9.25	5.00	7.61	2.96	7.08	9.78	7.32	6.93	9.33	11.35	4.47	2.34	5.39	2.28	2.25
Eu	3.73	3.56	2.36	1.70	2.70	1.24	2.32	3.42	2.52	2.33	3.37	3.67	1.52	0.81	1.80	0.91	0.86
Gd	11.87	11.42	7.44	5.60	8.70	2.69	7.95	11.25	8.24	7.60	9.77	12.45	6.04	3.33	6.64	3.27	3.28
Tb	1.52	1.45	1.09	0.80	1.07	0.36	1.02	1.55	1.13	0.98	1.21	1.37	1.07	0.60	1.07	0.62	0.62
Dy	6.43	6.22	7.10	3.40	4.82	2.06	4.36	6.83	4.84	4.30	5.12	5.71	5.96	3.62	5.77	3.75	3.66
Ho	1.13	1.11	0.77	0.60	0.93	0.36	0.76	1.21	0.86	0.72	0.84	0.91	1.35	0.80	1.17	0.83	0.81
Er	3.27	3.29	2.58	1.70	2.62	0.86	2.18	3.45	2.36	1.96	2.34	2.57	4.42	2.64	3.59	2.71	2.63
Tm	0.46	0.48	0.33	0.30	0.41	0.09	0.30	0.50	0.32	0.28	0.31	0.33	0.78	0.44	0.57	0.47	0.45
Yb	2.38	2.49	3.38	1.20	2.21	0.50	1.50	2.57	1.62	1.32	1.58	1.54	4.16	2.40	2.99	2.62	2.51
Lu	0.33	0.35	0.54	0.20	0.33	0.10	0.22	0.35	0.23	0.19	0.21	0.21	0.65	0.37	0.42	0.40	0.39
Total REE	302.18	311.70	330.81	97.30	275.97	65.66	195.47	246.28	171.17	178.52	258.41	360.63	115.25	49.43	101.68	34.20	34.26
(La/Yb) _n	18.71	19.28	17.26	11.21	21.31	18.49	19.75	12.94	13.36	18.22	25.96	37.02	3.30	1.95	3.12		
Nb/Y	3.21	3.29	3.33	12.51	0.51	1.01	2.85	2.04	2.28	2.85	4.10	5.27	0.48	0.24	0.47		
Nb/Zr	0.35	0.30	0.34	0.20	0.04	0.14	0.33	0.23	0.24	0.27	0.34	0.42	0.12	0.08	0.09		
⁸⁷ Sr/ ⁸⁶ Sr	0.70459±5	0.70472±1															
measured																	
⁸⁷ Sr/ ⁸⁶ Sr initial	0.7	0.7															
¹⁴³ Nd/ ¹⁴⁴ Nd	0.51	0.51															
measured																	



1.Picro-Basalt; 2.Basalt; 3.Basaltic Andesite; 4.Andesite; 5.Dacite; 6.Trachy Basalt;
7.Basaltic Trachy Andesite; 8.Trachy Andesite; 9.Trachydacite; 10.Tephrite Basanite;
11.Phono Tephrite; 12.Tephri-Phonolite; 13.Phonolite; 14.Trachyte; 15.Foidite;
16.Rhyolite.

Fig. 4. Total alkali–silica diagram (Le Bas and Streckeisen, 1991) for Kutch magmatic rocks. Analytical data of representative samples are given in Table 2. Full analytical data can be obtained from the supplementary database of the Journal.

268 suggest fractionation of olivine and clinopyroxene.
269 Among the Island Belt rocks, Σ REE in the Sadara
270 samples ($n=7$) varies between 160 and 187 ppm and
271 $(La/Yb)_n$ varies between 11.47 and 11.94. There is no
272 discernible Eu anomaly in any of the samples (Fig. 7b).
273 Σ REE in the Kaladongar dykes (224–355 ppm) is
274 higher than that in Kuran gabbro (72 ppm). These mafic
275 dykes have a fractionated REE pattern, $(La/Yb)_n$ vary-
276 ing from 13 to 21 in contrast to $(La/Yb)_n$ values around
277 5 in Kuran gabbro (Fig. 5f). It is clear that both the
278 Kaladongar dykes and Kuran gabbro are LREE enriched
279 (Fig. 7b).

280 As the Nir Wandh complex contains a number of
281 rock types, it is instructive to compare the trace element
282 behaviour patterns among them to explore genetic
283 evolution. In bivariate plots of some major and trace
284 elements (Fig. 6a–f) a scatter of points is observed for
285 the Nir Wandh rocks suggesting that a simple fractional
286 crystallisation model is not applicable. Σ REE in the
287 rocks of the Nir Wandh complex varies from 65.7 to
288 509.4 ppm from pyroxenite through gabbro to lampro-
289 phyre (camptonite). $(La/Yb)_n$ varies from 7.34 to 40.4.
290 All the rock types have fractionated REE patterns except
291 the diorites that have an unfractionated HREE or even a
292 slight enrichment of Yb and Lu. The primitive mantle

293 normalised (Sun and McDonough, 1989) trace element
294 patterns (Fig. 7a) for the Kaladongar dykes and Kuran
295 gabbro show positive Ba, Nb, Sr and Zr spikes. The
296 incompatible elements are enriched compared to the
297 primitive mantle and increase from Kuran gabbro
298 through Sadara sill to Kaladongar dykes. In chondrite
299 normalised REE plots (Fig. 7b), the Kaladongar dykes
300 are more fractionated than the Sadara sill and the Kuran
301 gabbro. The chondrite-normalised REE pattern of aver-
302 age Deccan tholeiite (Mahoney et al., 2000) is very
303 similar to that of the Kuran gabbro (Fig. 7b).

304 In chondrite-normalised REE plots of the fields of the
305 Nir Wandh rocks (Fig. 8), the gabbro field encompasses
306 those of the other rocks suggesting protracted crystal-
307 lisation. Lamprophyre and mafic dykes have more
308 fractionated and higher Σ REE abundances than the
309 pyroxenite, believed to be the basal member of the
310 complex. The light REE in the lamprophyres of Nir
311 Wandh are much less (La: 22 to 66 ppm) compared to
312 the La abundance of 174 ppm (sample no Yb-1) in the
313 lamprophyres of Murud–Janjira, south of Mumbai, also
314 in the Deccan Volcanic Province (Dessai et al., 1990)
315 (see Fig. 1 for location).

316 On MORB-normalised plots (Fig. 9a) the Nir Wandh
317 lamprophyre shows enrichment of LIL elements but 317

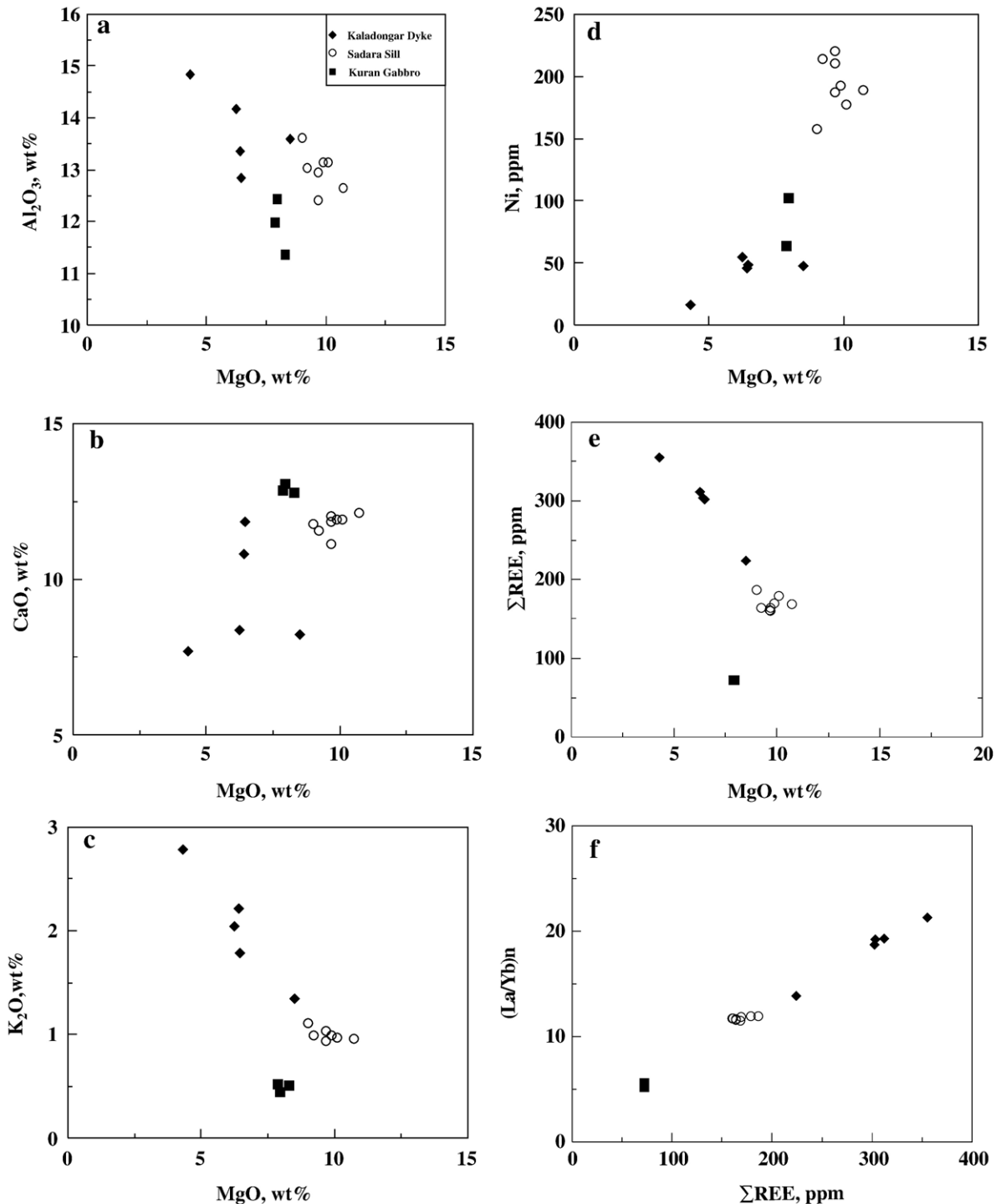


Fig. 5. Bivariate diagram showing Al_2O_3 , CaO, K_2O , Ni, ΣREE against MgO for Island Belt rocks, Kutch. In Fig. 5c and e, a negative correlation exists between K_2O and MgO and between ΣREE and MgO respectively. In both the diagrams, Kuran gabbro does not conform to the general trend. A significant positive correlation exists between $(La/Yb)_n$ and ΣREE among all the rock types (Fig. 5f).

318 compatible and HFS elements show MORB-like levels.
 319 In contrast, the camptonites of Murud–Janjira of
 320 Bombay coast and Gondwana lamprophyres of eastern

India (JC-2) (Fig. 9) show strong enrichments of LIL
 321 elements as are typical of alkaline lamprophyres and
 322 nephelinites (Le Bas, 1987; Dessai et al., 1990; Rock
 323

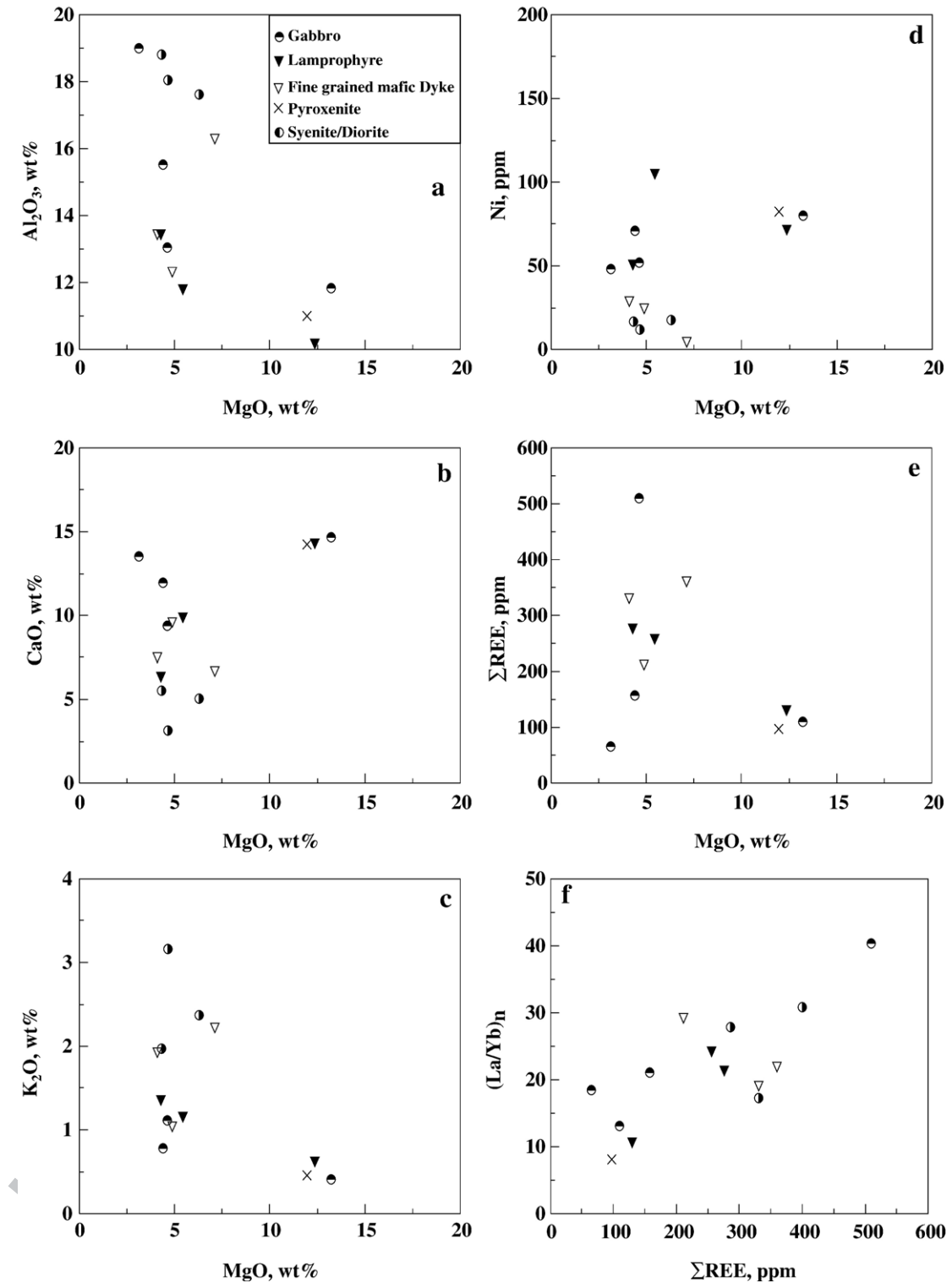


Fig. 6. Variation diagrams of selected major and trace elements against MgO for constituent rocks of the Nir Wandh Igneous complex. Pyroxenite (NW 85), gabbro (NW 5) and lamprophyre (NW 77D) have high MgO compared to the other samples and fall away from the general trends.

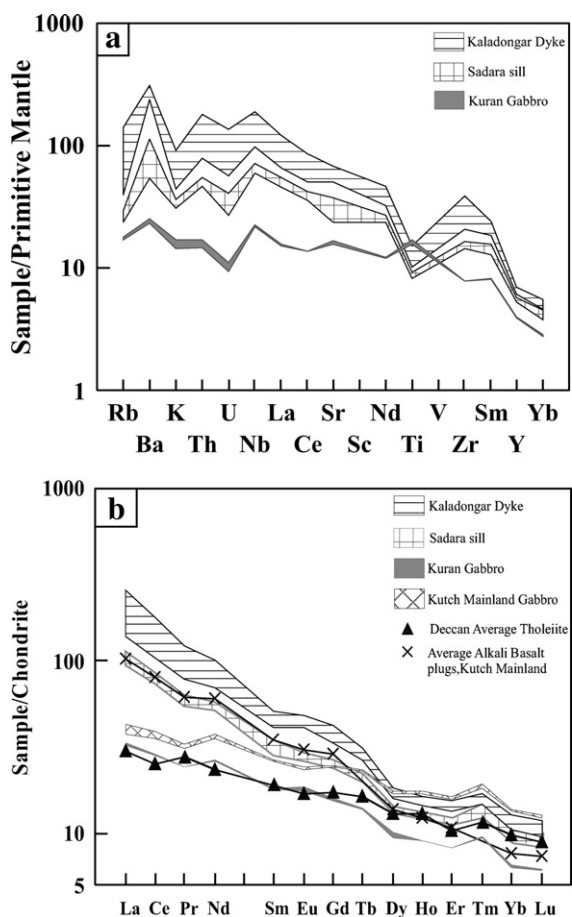


Fig. 7. a: Primitive mantle-normalised trace element patterns (after Sun and McDonough, 1989) for the Island belt rocks. A general similarity among Kaladongar dykes, Sadara sill and Kuran gabbro is seen although there is a significant variation in the incompatible trace element abundances. b: Chondrite-normalised REE patterns for the Island rocks along with the pattern for average Deccan tholeiites (Mahoney et al., 2000); average alkaline basalt and gabbro are from Mainland (this study). Chondrite abundance values are from Evensen et al. (1978).

et al., 1992). These could reflect not only the nature of the enriched source rock as commonly assumed for lamprophyric rocks (see Rock et al., op. cit., for example) but also of the processes of magma generation and subsequent modification by fractional crystallisation.

The variation of Al_2O_3 , CaO and K_2O with MgO in the Kutch Mainland magmatic rocks (Fig. 10a–c) show scatter, but Ni (Fig. 10d) maintains a good positive correlation as in the Island Belt rocks. Similarly $(La/Yb)_n$ and ΣREE also has a good positive correlation (Fig. 10f). A role of fractional crystallisation of olivine is clearly indicated. The primitive mantle normalised trace element abundances in alkali basalt, tholeiite and gabbro of Kutch Mainland are similar (Fig. 11a). This pattern is

also maintained in the chondrite-normalised REE abundances (Fig. 11b). Plots of Ba and Rb against TiO_2 for the alkali basalts of Kutch Mainland show a continuous variation of TiO_2 from 2.15 to 3.55 wt.% but both Ba and Rb remain more or less constant up to about 2.8 wt.% TiO_2 (Fig. 12). Thereafter, both Ba and Rb increase with increasing TiO_2 . The basaltic flows of the Deccan Volcanic Province have been classified into Formations based on geochemical criteria (Cox and Hawkesworth, 1985; Beane et al., 1986). Key criteria in the Western Ghats include Sr, Ba, Rb, TiO_2 , and Zr/Nb ratios (Lightfoot et al., 1990). Data for the tholeiitic basalt samples of this study (supplementary data base) show high Ba concentrations (182–315 ppm), restricted Sr (211–241 ppm), Rb (24.5–38.6 ppm), low Zr/Nb (2.9–8.1) and low TiO_2 (1.55–2.99 ppm). These characteristics are different from those of the basaltic flows of Mahabaleshwar region (Cox and Hawkesworth, 1985). The criteria used for the classification of the Western Ghats volcanic rocks do not hold in other areas of DVP (Mahoney et al., 2000). Melluso et al. (2006), among others, have shown important lateral heterogeneities in the mantle and a break from the Western Ghats to Gujarat. Therefore, the petrochemical variation observed in the Kutch volcanic rocks is not surprising.

4. Isotopic composition of Sr and Nd

Isotopic measurements were performed on a Thermo Electron TRITON fully automatic variable multi collector mass spectrometer at the Indian Institute of Technology, Roorkee. During the period of analysis, SRM-987 isotopic standard gave a $^{87}Sr/^{86}Sr$ value of

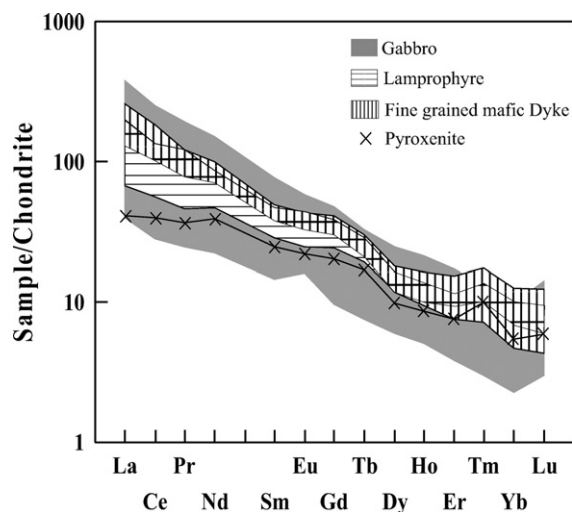


Fig. 8. Chondrite-normalised REE abundances for Nir Wandh rocks. Chondrite abundance values are from Evensen et al. (1978).

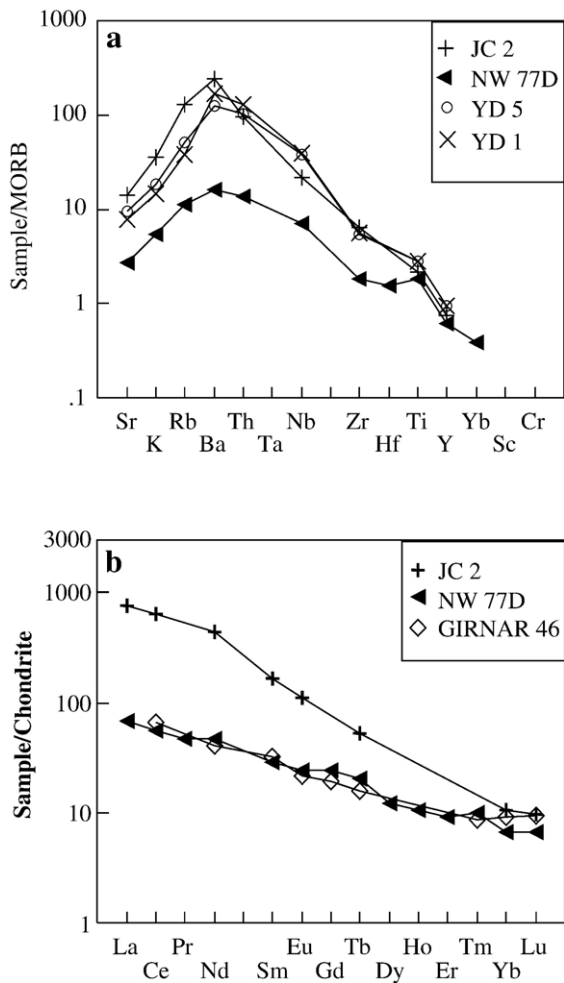


Fig. 9. a: MORB-normalised patterns of selected incompatible trace elements of Nir Wandh lamprophyre (sample no NW 77D) compared with camptonite from Murud, Bombay coast (sample no YD1, YD5; Dessai et al., 1990) and minette (sample No JC 2; Rock et al., 1992) using Pearce's (1983) element order and normalizing values. b: Chondrite-normalised rare earth element pattern of the Nir Wandh lamprophyre (NW 77D; data from supplementary database) compared with that of minette (JC 1) from the Jharia coalfield, India (Rock et al., 1992) and lamprophyre from the Girnar Igneous Complex (Girnar 46; Paul et al., 1977). Normalising values are from Evensen et al. (1978).

369 0.710248 + 10 (1 s.e., $n=55$) and Ames Nd standard gave
 370 a $^{143}\text{Nd}/^{144}\text{Nd}$ value of $0.512138 + 4$ (1 s.e., $n=41$). The
 371 error assigned is 0.05% for $^{87}\text{Sr}/^{86}\text{Sr}$ and 0.01% for
 372 $^{143}\text{Nd}/^{144}\text{Nd}$ measurement. The analytical details in
 373 respect of the Kutch samples are given in Das et al.
 374 (in press).

375 Measured $^{87}\text{Sr}/^{86}\text{Sr}$ ratios in the five mafic dyke
 376 (Kaladongar) samples vary from 0.70428 to 0.70593;
 377 $^{87}\text{Rb}/^{86}\text{Sr}$ ratios are low (0.016 to 0.127). No isotopic
 378 age data is available for the northern Island Belt mag-
 379 matic rocks. However, assuming an age of 65 Ma

(equivalent to Deccan volcanism), the initial $^{87}\text{Sr}/^{86}\text{Sr}$ 380
 ratios are found to vary from 0.70419 to 0.70589. In 381
 contrast, $^{87}\text{Sr}/^{86}\text{Sr}$ ratios in two Kuran gabbro samples 382
 are 0.70409 and 0.71065 (see supplementary database; 383
 Das et al., in press). The ϵNd (i) values of the dyke 384
 samples vary from +0.3 to -6.5. 385

In the plot of $^{143}\text{Nd}/^{144}\text{Nd}$ vs. $^{87}\text{Sr}/^{86}\text{Sr}$ ratios 386
 (Fig. 13), besides the Kutch samples, the Bhuj basanites 387
 (Simonetti et al., 1998) and the Deccan basalts of 388
 Western Ghats (Lightfoot and Hawkesworth, 1988) are 389
 also shown. The Deccan basalts show a much larger 390
 spread in Sr–Nd isotopic composition with two distinct 391
 arrays. Among the different flows of Western Ghats, the 392
 Bushe flow has the most radiogenic $^{87}\text{Sr}/^{86}\text{Sr}$ and un- 393
 radiogenic $^{143}\text{Nd}/^{144}\text{Nd}$. This is believed to result from 394
 mixing between two end members, one Réunion like 395
 asthenospheric mantle and another with high $^{87}\text{Sr}/^{86}\text{Sr}$ 396
 but low $^{143}\text{Nd}/^{144}\text{Nd}$ (Lightfoot and Hawkesworth, 397
 1988). Among the samples of Kutch shown in Fig. 13, a 398
 majority has radiogenic $^{143}\text{Nd}/^{144}\text{Nd}$ but low radiogenic 399
 $^{87}\text{Sr}/^{86}\text{Sr}$, and fall near the Ambenali–Panhala–Réunion 400
 overlap. Even allowing for the small number of samples 401
 from Kutch, it is clear that these have a restricted Nd–Sr 402
 isotopic composition in the context of the Deccan 403
 basalts. Five samples of the Kaladongar dykes show a 404
 wide $^{143}\text{Nd}/^{144}\text{Nd}$ but restricted $^{87}\text{Sr}/^{86}\text{Sr}$. Comparison 405
 of the $^{87}\text{Sr}/^{86}\text{Sr}$ and the Mg # (Table 2) shows a positive 406
 correlation. The most radiogenic sample, BH 28.2 with 407
 $^{87}\text{Sr}/^{86}\text{Sr}=0.70595$ is the most mafic (Mg # = 59). This 408
 is similar to the Bushe but unlike the Ambenali 409
 characters. The Kaladongar dyke isotopic composition 410
 is likely to be the result of mixing between a Réunion 411
 like composition and another component with radio- 412
 genic $^{87}\text{Sr}/^{86}\text{Sr}$ and unradiogenic $^{143}\text{Nd}/^{144}\text{Nd}$. 413

The Sr–Nd isotopic compositions of the Kutch sam- 414
 ples of the present study and the basanites of Simonetti 415
 et al. (1998) seem to reflect a lateral heterogeneity from 416
 the Western Ghat Trap mantle to Kutch. From trace 417
 element enrichment of high-Ti picrites of Gujarat, 418
 Melluso et al. (1995) came to a similar conclusion. 419
 The Bhuj basanites have lower initial $^{87}\text{Sr}/^{86}\text{Sr}$ ratios 420
 (0.70357 to 0.70396) and higher initial $^{143}\text{Nd}/^{144}\text{Nd}$ 421
 ratios (0.51281 to 0.51287) compared to the Kaladongar 422
 dykes in northern Island Belt. Therefore, the source 423
 region for the northern Island Belt rocks would have 424
 been enriched in Rb/Sr and Sm/Nd ratios. 425

5. Paleomagnetic results 426

Paleomagnetic investigations comprising AF and 427
 thermal demagnetisations were carried out on 150 ori- 428
 ented block samples (around 900 cylindrical specimens 429

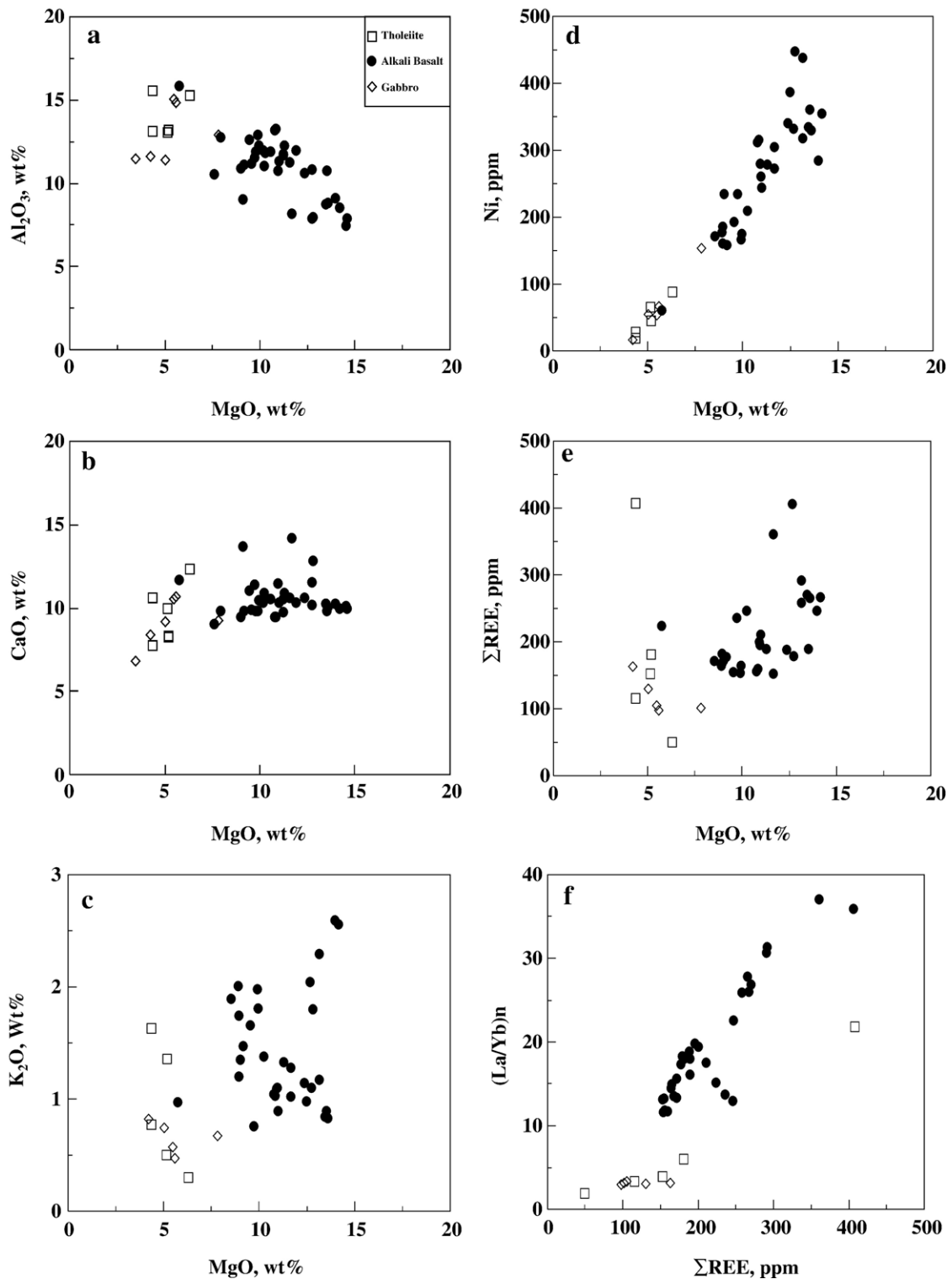


Fig. 10. Variation diagrams of selected major and trace elements against MgO for the rocks of the Kutch Mainland.

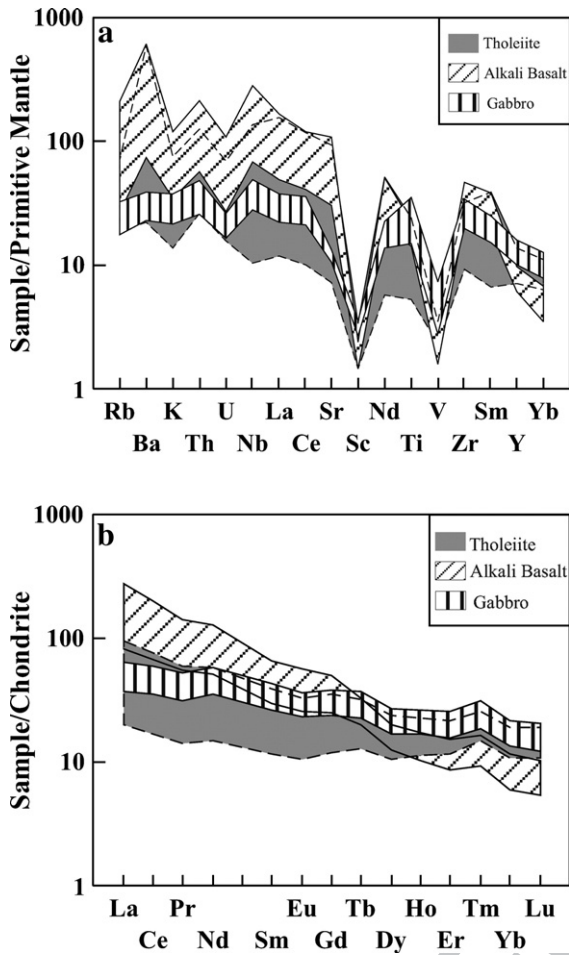


Fig. 11. a: Primitive mantle-normalised trace element patterns (after Sun and McDonough, 1989) for the major rock types of Kutch Mainland. Note the similarity of the distribution patterns. b: Chondrite-normalised REE patterns for the Kutch mainland rocks. Chondrite abundance values are from Evensen et al. (1978).

of 2.5 cm diameter \times 2.2 cm length) collected from 30 magmatic bodies/sites (sills, dykes, plugs and flows). Natural Remanent Magnetization (NRM) directions were measured by a JR-5 spinner magnetometer (AGICO, Czech Republic). AF and thermal demagnetizations were carried by a Molspin (UK) AF demagnetizer and MITD-800 thermal demagnetizer (Germany), respectively. Magnetic susceptibilities of the specimens were measured by a MS-2 (Bartington, UK) susceptibility meter.

Based on their spatial proximity, geochemical signatures and mineralogical characteristics, the magmatic bodies were distributed into three groups.

The first group consists of Mainland tholeiite flow sites (Dhanoi, Dhanoi–Dahisara and Pranpur) and Main Land Gabbroic intrusives sites (Kaya Dongar, Likhi

Hill, Lakhpa–Khatieu, Dhar Dongar, Ranadada dyke, Habo Dome and Chitrod). The mean Magnetic Susceptibility (MS) values for the tholeiites and intrusives were found as $25,073 \times 10^{-6}$ and $32,065 \times 10^{-6}$ SI respectively. The mean NRM intensities for the flows and intrusives were noted as 9 A/m and 4.58 A/m respectively, whereas the calculated Q-ratios (Koingsberger ratio) for tholeiites and dykes were observed as 10.98 and 5.33 respectively. The stability of the remanence directions in the samples were tested by the application of stepwise AF fields at 25, 50, 75, 100, 150, 200, 250, 300, 350, 400, 450, 500, 600, 800 and 1000 Oe and thermal steps of 100, 150, 200, 300, 400, 500, 530, 560, 580 and 600 °C. From the obtained AF and thermal

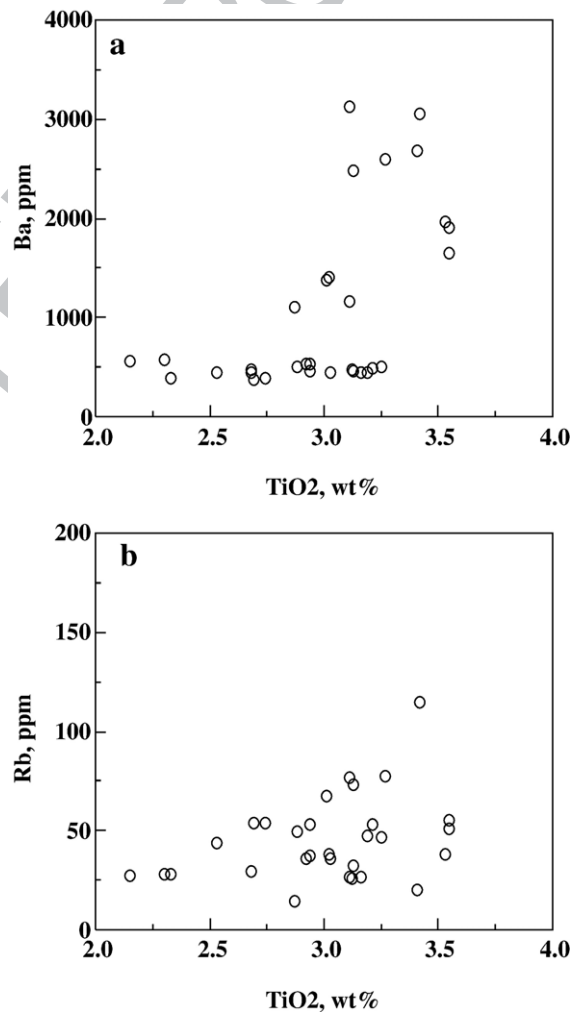


Fig. 12. Plot of Ba and Rb against TiO_2 of alkali basalt of Kutch mainland. A continuous variation of TiO_2 content from 2.15 to 3.55 wt.% is visible. However, the samples can be classified as a high- TiO_2 (>3 wt.%) and low- TiO_2 (<3 wt.%) group. See text for grouping on the basis of other trace elements.

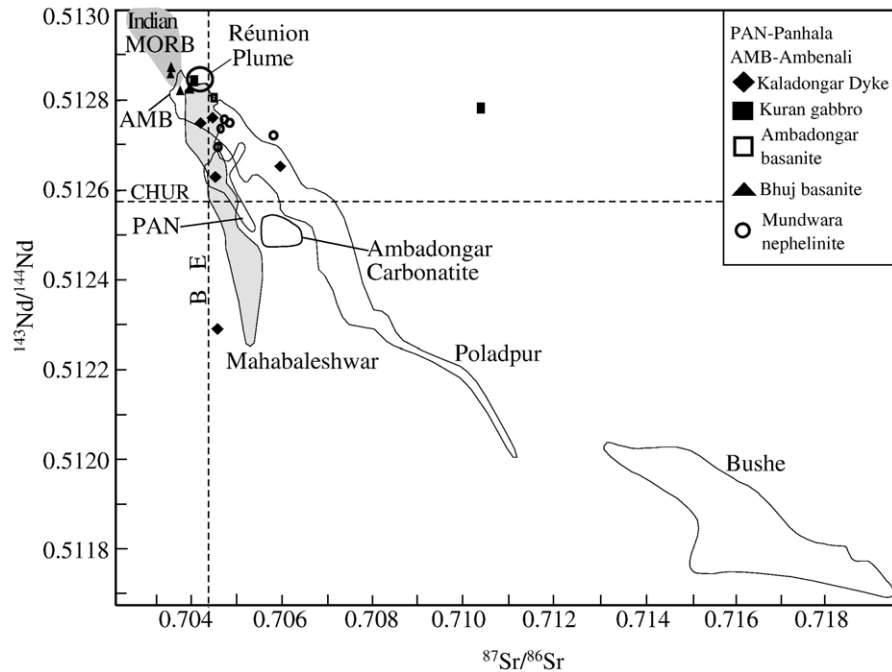


Fig. 13. Nd vs Sr isotope plot for Kaladongar dyke and Kuran gabbro of Kutch (Data: Das et al., in press). Source of other data: Deccan basalt (Lightfoot and Hawkesworth, 1988) Bhuj Basanite (Simonetti et al., 1998). Other fields in this figure are reproduced from Simonetti et al. (1998).

demagnetization spectra, the Characteristic Remanent Magnetization (ChRM) directions were recovered at 250–400 Oe peak AF fields and at 400–560 °C thermal steps. In this group, five intrusive bodies showed ‘normal polarity’ (north-west declinations associated with moderate negative inclinations) and another two intrusives along with three-flow sites revealed a ‘reverse polarity’ direction (trending south-east declinations with moderate negative inclinations). From the complete AF and thermal cleanings on the samples of the first group sites, a mean ChRM direction was calculated by using the Fisher’s statistics (Fisher, 1953) and the ChRM was noted as $D=336$; $I=-41$ ($\alpha_{95}=13.95$; $k=12.95$; $n=10$ sites).

The alkali basalts of Kutch Mainland (12 sites representing Bhujia, Bharar, Kingriya Dongar, Vithon, Dinodhar, Ranadada, Wamoti Moti, Dhruvia Hill, Nana Dongar, Jawharnagar–Kanyaber and Lodai) form Group-II for paleomagnetic study. Magnetic susceptibilities of these sites were found in the range of 9912×10^{-6} SI to 69708×10^{-6} SI with a mean of 34068×10^{-6} SI. The mean NRM intensity and Q ratios were found as 9.27 A/m and 12.29 respectively. The viscous component was erased at and around the temperature of 200 °C and 50 Oe AF steps. The ChRMs were grouped well in the range of 350–530 °C and 50–500 Oe AF fields. Out of the twelve-alkalic

basaltic flows, normal polarity was recovered in seven sites and a reverse polarity was isolated in the remaining five sites. The mean ChRM of the second group sites was found as $D=336$; $I=-53$ ($\alpha_{95}=10.28$; $k=20.03$; $n=12$).

Eight sites representing the Kaladongar dyke swarm, Sadara sill, Kuran, Raimarlo Hill and Nir Wandh of the northern Island Belt form Group-III. For this group of samples, higher magnetic susceptibilities (with a mean as $53,036 \times 10^{-6}$ SI units) were observed in comparison to those of Group-I and II magmatic rocks. The mean NRM intensities and Q -ratios for this group were 4.63 A/m and 3.54 respectively, which were found to be lower than those of Group-I and Group-II rocks. The ChRM directions were recovered from all the eight sites through the application of AF and thermal demagnetizations of 400–600 Oe and 400–530 °C windows. From the analyses of the demagnetization data sets, it was observed that two sites (Kuran and Kaladongar) showed a reverse polarity and the other six sites exhibited normal polarity. Normal and reverse polarity signatures in the Kaladongar sites indicate multiple intrusive events for the dykes in Kaladongar. The mean ChRM for the third group was recorded as $D=336$; $I=-40$ ($\alpha_{95}=10$; $k=31.4$; $n=8$).

Antipodal nature of isolated normal ($D=332$, $I=-50$, $\alpha_{95}=8.23$; 18 sites) and reverse ($D=157$, $I=41$, 13

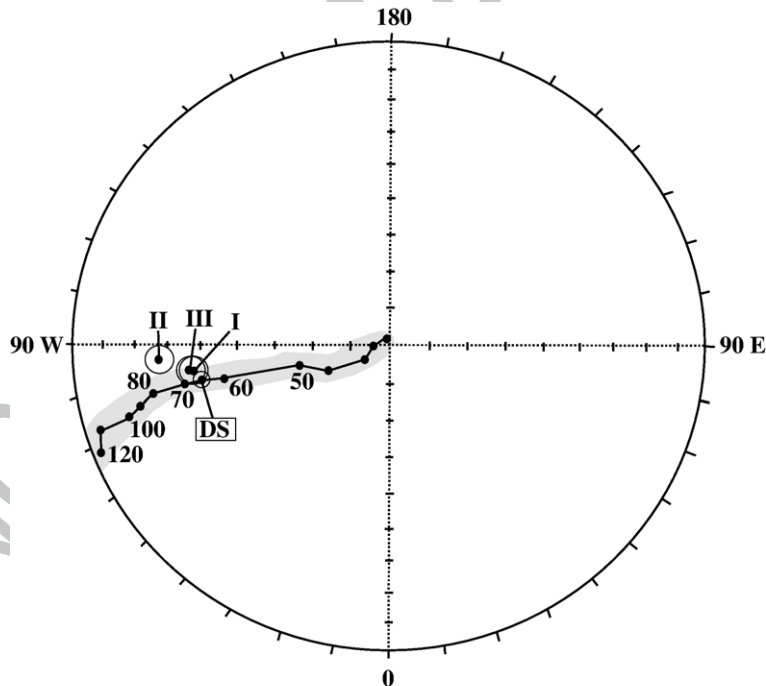
514 $\alpha_{95}=11.29$; 12 sites) polarity directions from the studied
 515 30 sites indicate that the isolated ChRM directions were
 516 of primary nature and statistically significant. By con-
 517 verting the reverse polarity directions to normal, the
 518 overall mean of all the sites calculated by using the
 519 Fisher's statistics was found as $D=335^\circ$; $I=-45^\circ$ ($\alpha_{95}=
 520 7.5$; $n=30$ sites) and the corresponding Virtual Geo-
 521 magnetic Pole (VGP) at 33.7°N and 81.2°W ($dp/
 522 dm=5.81/9.18$). The obtained pole was found statisti-
 523 cally concordant with that of the Deccan Super pole
 524 (36.9°N ; 78.7°W) as reported by Vandamme and
 525 Courtillot (1992). This suggests that the studied Kutch
 526 basin magmatic events belong to chrons 30N–29R–
 527 29N. However, older ages of the order of 1–2 Ma could
 528 be assigned to these magmatic bodies relative to the
 529 peak of the Deccan magmatic event of 65 Ma, as there is
 530 a 3° difference between the VGP latitude of the samples
 531 of the present study and the Deccan Super pole VGP
 532 latitude. Further, we have calculated VGPs for the
 533 three groups separately. The VGPs for the three groups
 534 were found as: 37.6°N : 277.4°W (for Group-I),
 535 27.8°N : 273.2°W (for Group-II) and 37°N : 277°W (for
 536 Group-III). The obtained VGPs are plotted along with
 537 the Deccan Super pole (Vandamme et al., 1991) on the

synthetic APWP (Apparent Polar Wandering Path) in 538
 Fig. 14. From the figure it can be observed that Group-I 539
 and Group-III magmatic rocks (Kutch Mainland 540
 tholeiites and gabbroic dykes and the northern Island 541
 Belt) and the Deccan Super (DS) pole were grouped at 542
 the 65 Ma part of the synthetic APWP. However, the 543
 Group-II (alkali basalts) VGP was found around 70– 544
 75 Ma part of the synthetic APWP, indicating that these 545
 Group-II rocks are relatively older than the Group-I and 546
 Group-III rocks. Available ^{39}Ar - ^{40}Ar ages of the 547
 tholeiites are 65 Ma against the ages of 68 Ma for the 548
 alkali basalts (Pande et al., 1988). However, absolute 549
 age determinations of the Kutch magmatic bodies will 550
 be helpful in determining the span of the magmatic 551
 episodes. 552

6. Discussion 553

6.1. General comparison of the magmatic rocks of 554 northern Island Belt and Kutch Mainland 555

Significant variation among the magmatic rock types 556
 such as alkali basalt, picrite and differentiated mafic 557
 complexes in Gujarat compared to the overall tholeiitic 558



Group-I: Tholeiites and gabbroic dykes of Kutch Mainland
 Group-II: Alkali basalt plugs of Kutch Mainland
 Group-III: Magmatic rocks of northern Island Belt

Fig. 14. Groups I, II and III Kutch magmatic bodies and Deccan Super pole (DS) VGPs are plotted along with the synthetic APWP for India (Vandamme et al., 1990).

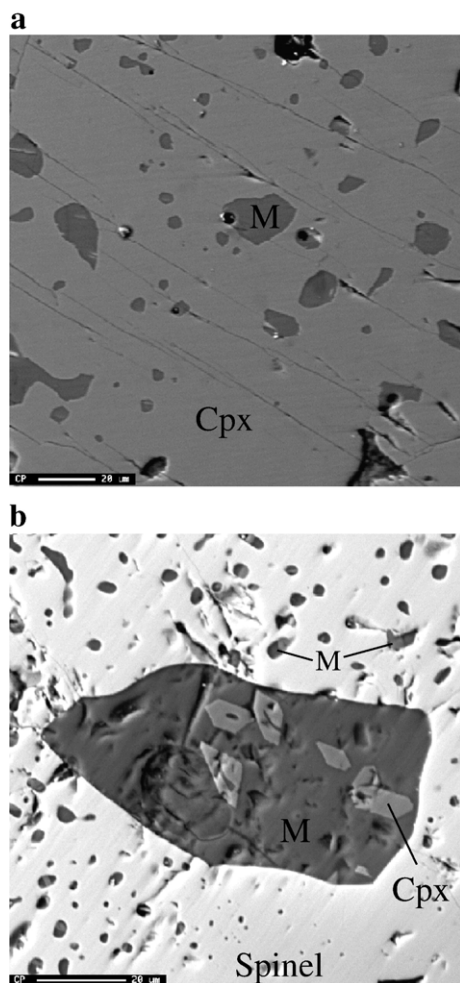


Fig. 15. Photomicrographs showing melt inclusions in ultramafic xenolith minerals. **a** shows melt inclusions in clinopyroxene in ultramafic xenoliths. **b** shows melt in spinel. Note that small Cpx grains have crystallized out from the large melt inclusion.

559 nature of the Deccan Volcanic Province has been noted
 560 earlier (Krishnamurthy and Cox, 1977; Mahoney, 1988;
 561 Melluso et al., 2006). The present study has further
 562 documented the occurrences of mildly alkaline gabbro,
 563 basanite, and camptonite from Kutch northern Island
 564 Belt. Admittedly, between the northern Island Belt and
 565 the southern Kutch Mainland there is a stretch of 80 km
 566 with no magmatic rock exposure. However, when we
 567 compare the general chemical features of these two belts
 568 (Fig. 7b) we note that the chondrite-normalised REE
 569 plots for Sadara sill (data from Ray et al., 2006) and the
 570 alkali basalt plugs are similar. Between the Kutch
 571 Mainland gabbro and Kuran gabbro (northern Island
 572 Belt) the REE abundances are similar although the
 573 Kutch Mainland gabbro is enriched suggesting that they
 574 were derived from similar source in the mantle. Taking

the threshold values of 3 wt.% for TiO₂, 1000 ppm for
 575 Ba and 50 ppm for Rb, it is observed that the alkali
 576 basalt plugs belong to a high-TiO₂, high-Ba and high-Rb
 577 (e.g. Lodai, Bhujia, Dhrubia, Bharar, Kingriya), a low-
 578 TiO₂, low-Ba and a low-Rb (e.g. Jaksh, Nakhatrana,
 579 Dinodhar) group (see Fig. 2a for location of the plugs).
 580 Geographically, the former group is in eastern Kutch
 581 while the latter is in its western part. The frequency and
 582 size of the ultramafic xenoliths are larger in the eastern
 583 plugs. 584

Our paleomagnetic studies indicate that the Group-I
 585 and Group-III magmatic rocks (Kutch Mainland Tho-
 586 leiitic basalts and the gabbroic dykes and northern
 587 Island Belt rocks) are grouped at one place and match
 588 well with that of the Deccan Super pole. The VGP of the
 589 alkali basalts of Kutch Mainland (Group-II rocks) match
 590 with the 70–75 Ma part of the APWP (Vandamme et al.,
 591 1991). From this, it has been inferred that the Kutch
 592 Mainland alkali basaltic plugs of the studied region are
 593 relatively older than those of the northern Island and
 594 Kutch Mainland tholeiite and gabbroic bodies. Only
 595 absolute age determinations will constrain the conclu-
 596 sions decisively. 597

The geological setting of the Kutch basin has clearly
 598 been demonstrated to form as a consequence of rifting
 599 (Biswas, 2005). In common with other continental rifts,
 600 the magmatic rocks in Kutch constitute a small part of
 601 the basin. To draw a parallel, in Kenya, for example,
 602 tectonic evolution began with the development of a
 603 shallow basin in the Turkana region in the north in Early
 604 Miocene (Baker, 1987). Tectonic development of the
 605 Kenya rift is usually divided into pre-rift (30–12 Ma
 606 BP), half-graben (12–4 Ma BP) and graben stages of
 607 development. The nature of volcanism changed from
 608 nephelinite–carbonatite through alkali basalt to phono-
 609 lites. The rock types in the Kutch basin are not as varied.
 610 However, in the Kutch region, there is a petrological
 611 zonation, north to south, from alkaline intrusives, alka-
 612 line basalt plugs to tholeiites. The emplacement of the
 613 intrusives in the north has been controlled by the pre-
 614 existing rift-related faults. 615

6.2. Petrogenesis 616

Within the Deccan Volcanic Province, the Gujarat
 617 area in its northwestern part exposes a wide range of
 618 rock types ranging from picro-basalts to rhyolites
 619 (Krishnamurthy and Cox, 1977; Melluso et al., 1999,
 620 2006). Four distinct petrographic and geochemical
 621 magma groups having variable TiO₂ were identified. It
 622 was suggested that these were derived from different
 623 mantle sources and that there is a strong lateral
 624

625 heterogeneity in the mantle, possibly HFSE depleted,
626 beneath Gujarat (Melluso et al., 1999).

627 Further to the west of Kathiawar in Gujarat, there are
628 also alkaline volcanic rocks, which have recently drawn
629 the attention of many petrologists (Krishnamurthy and
630 Cox, 1977; Melluso et al., 1995; Simonetti et al., 1998;
631 Melluso et al., 2006). The narrow belt of tholeiitic rocks
632 skirting the coast of Kutch has been linked to the Deccan
633 volcanic rocks. However, the alkali basalts and gabbros
634 of the northern Island Belt in Kutch, described in an
635 earlier section, have not been studied earlier except by
636 Maitra (2003). Guha et al. (2005) linked the alkali
637 basalts of Kutch Mainland to the rifting of the Kutch
638 basin. The presence of ultramafic xenoliths in the alkali
639 basalt plugs of Kutch has been mentioned earlier.
640 Karmalkar and Rege (2002) described the petrology of
641 these xenoliths and presented geochemical data of the
642 chromium diopsides from the xenoliths. The depletion
643 of Al, Ti, Ga, Y and HREE with increasing Mg# in
644 diopside, the increase in Ni and Ni/Co with increasing
645 Mg# in olivine and increase in Cr/Al of spinels were
646 believed to be the result of extraction of melt from the
647 source region. Very high concentrations of incompatible
648 elements including LREE in these ultramafic xenoliths
649 reflect an enriched source.

650 The tholeiite–alkali basalt association in continental
651 flood basalt province has been discussed (Bose, 1980;
652 Devey and Stephens, 1991; Sheth and Chandrasekharan,
653 1997). The alkaline complexes in the Deccan Volcanic
654 Province occur mostly along the rift zones (Sheth and
655 Chandrasekharan, 1997). The sediment column in the
656 Kutch basin represents the time span from Middle
657 Jurassic to Recent and shows fluvial to marine facies
658 with rapid variation of thickness of sediments. The alkali
659 basalt intrudes this sediment column. Near Nakhatrana
660 (Fig. 2a), Guha et al. (2005) recorded the presence of
661 tholeiitic flows over alkali basalt. In the northern end of
662 the Cambay Graben, Basu et al. (1993) obtained
663 $^{39}\text{Ar}/^{40}\text{Ar}$ ages of 68.53 to 68.57 Ma for biotites from
664 alkaline olivine gabbro (Mundwara Complex) and from
665 alkali pyroxenite (Sarnu–Dandali Complex). This estab-
666 lished that the alkali basalt magmatism in Kutch
667 preceded the major tholeiite magmatism of the coastal
668 belt, which is believed to have extruded at 65 Ma.

669 Although Devey and Stephens (1991) concluded that
670 large quantities of tholeiite followed by alkali basalt
671 could be generated by varying degrees of partial melting,
672 numerous studies (Francis and Ludden, 1990; Pilet,
673 2001; Larsen et al., 2003) have emphasized the signif-
674 icance of “metasomatism” for generation of alkali basalt.
675 Mantle-derived ultramafic xenoliths from kimberlites
676 and alkali basalts have documented evidence of infil-

677 tration of melts/veins from the deeper asthenosphere,
678 which got frozen at upper levels causing variable enrich-
679 ment (Erlank et al., 1987). Modal metasomatism records
680 textural change along with formation of hydrous
681 minerals such as phlogopite and kaersutite. However,
682 when the volume of infiltrating melt is low, cryptic
683 metasomatism along with enrichment of selective in-
684 compatible elements takes place (Lee et al., 1996;
685 Downes et al., 2004). Selective melting of such enriched
686 zones can generate the Kutch alkali basalt with the
687 observed geochemical characteristics. The geochemical
688 characters discussed earlier have indicated that crystal
689 fractionation, including accumulation of various phases
690 such as clinopyroxene, and olivine has an important role
691 in the formation of the alkaline rocks such as noticed in
692 the Nir Wandh complex.

693 Silica-saturated, alkali and alumina rich glasses
694 (Fig. 15) are found within clinopyroxene and spinel of
695 wehrlite and lherzolite xenoliths of the Kutch alkali
696 basalt. Karmalkar and Sarma (2003) attributed forma-
697 tion of the silicate glass to the interaction of carbonatitic
698 and silicate fluid coming from the asthenospheric
699 mantle with the orthopyroxene of lithospheric mantle
700 lherzolite. The process has been described as wherlitisa-
701 tion (Yaxley et al., 1997). It is generally agreed that Si–
702 Na–K rich glasses represent a type of metasomatic agent
703 circulating in the upper mantle (Edgar et al., 1989;
704 Draper, 1992). From the geochemical studies of spinel
705 lherzolite xenoliths of Kutch, Karmalkar and Rege
706 (2002) concluded that the lithospheric mantle acquired
707 distinctive features such as LREE enrichment, high Zr/
708 Hf, La/Yb and Nb/La and low Ti/Eu due to interaction
709 of carbonatitic melt and peridotite. We found phlogo-
710 pite, apatite and calcite in the xenolith fragments and
711 veins of calcite in between olivine and clinopyroxene in
712 wehrlite xenolith. This mineral association further
713 strengthens the idea that an episodic metasomatism
714 occurred in the lithospheric mantle beneath Kutch.
715 Metasomatism was brought about by alkali rich silicate
716 and carbonatitic fluid. The P–T estimate of equilibration
717 from coexisting orthopyroxene-clinopyroxene in spinel
718 lherzolite is of the order of 980°–1060 °C and 9–12 Kb
719 (Mukherjee and Biswas, 1988; Karmalkar et al., 2005).

670 6.3. Magma emplacement 720

721 The rifted nature of the Kutch basin has been docu-
722 mented from stratigraphic and tectonic studies (Biswas,
723 2005). The rifting and the attendant extension of the
724 Kutch basin may be attributed to thermal thinning of the
725 lithosphere similar to that advocated for the Cenozoic
726 European Rift System (Dèzes et al., 2004). It should be

noted that in Kutch there is no magmatic activity in the Early Jurassic when rifting was initiated. Magmatic activity in Kutch was initiated much later. For the melting process to begin, mantle temperature has to be raised above the solidus. This is possible either by asthenospheric up welling or by increased temperature input from a mantle plume.

Various authors have hypothesized that the Réunion plume was generally located at the junction of Cambay rift, Son rift and the Western Ghat rift in western India (Fig. 1) at the time of the main phase of Deccan volcanism (Sen and Cohen, 1994) whose remaining ‘tail’ is now causing volcanic eruptions on the Réunion Island (Duncan, 1978; Richards et al., 1989; Campbell and Griffiths, 1990). The temperature gradient of the plume head would decrease away from the head, 800–1000 km (Sen and Cohen, 1994; Kerr, 2003) across. If this hypothesis is correct, low temperature fusible constituents in the Kutch lithospheric mantle would have melted first leading to the formation of the low volume alkaline basalt magma in Kutch. Tholeiitic basalt formed later (ca. 3 Ma) due to higher degree of melting. Bouguer gravity data (Raval, 2001) suggest ~~under plating~~ of high-density material perhaps in the form of a large magmatic body in the deep crust close to the mantle in Kutch–Saurashtra–Cambay region (Fig. 1). Such a magmatic body is believed to be the remnant of the lithospheric melt that formed during rift climax (Biswas, 2005). Emplacement of these magmatic bodies in the northern Island Belt took place along the major rift-bounding faults (Fig. 2b) in Late Cretaceous.

7. Conclusions

- i. The tholeiitic basalts of southern Kutch have petrological and geochronological similarity with the main eruptive phase of the Deccan Volcanic Province and are considered as the earliest eruptive phase. Hence the mineralogical and geochemical features of these rocks document the onset of volcanism in the Deccan Volcanic Province.
- ii. Alkali basalt and alkaline intrusive rocks occur in the central and northern part of the Kutch rift basin. Occurrence of voluminous alkaline rocks as in the present study area is unique in the whole DVP.
- iii. Paleomagnetic data indicate close temporal relation between these alkaline rocks and the tholeiitic basalts.
- iv. Mineralogical studies and composition of melt inclusions in ultramafic xenoliths (Karmalkar and Rege, 2002; Karmalkar and Sarma, 2003) from the Kutch Mainland alkali basalts indicate that carbona-

titic and silicate fluid pervaded the Kutch lithosphere. Low degree partial melting of LILE-enriched lithosphere as a result of heat supply from the Réunion plume generated early primary alkaline magma. Fractionation of olivine and clinopyroxene induced subsequent chemical and mineralogical variation. v. The source rocks for the magmatic rocks of Kutch is different from the main DVP. This suggests a lateral heterogeneity in the mantle from the Western Ghats to Gujarat.

Acknowledgement

DKP is grateful to the Indian National Science Academy for a Senior Scientist’s position. We thank the Department of Science and Technology, Government of India for financial support, P.K. Govil and V. Balaram for analytical assistance and P. Dasgupta for comments on an earlier draft of the manuscript. B.C. Sarkar helped us in the data presentation, H.N. Bhattacharya, Head, Geology, Presidency College provided facilities for this research. Constructive comments from the Journal reviewers, P.R. Hooper, L. Vanderkluisen, an anonymous reviewer and Yigang Xu (editor) improved the clarity of the paper very significantly. Sweety Mazumdar helped in data presentation and Tom Bizley of Florida Center for Analytical Electron Microscopy helped with the BSE image.

Appendix A. Supplementary data

Supplementary data associated with this article can be found, in the online version, at [doi:10.1016/j.lithos.2007.08.005](https://doi.org/10.1016/j.lithos.2007.08.005).

References

- Baker, B.H., 1987. Outline of the petrology of the Kenya rift alkaline province. In: Fitton, J.G., Upton, B.G.J. (Eds.), *Alkaline Igneous Rocks*. Geological Society Spec. Publ., vol. 30, pp. 293–311.
- Balaram, V., Rao, G., Gnanaswar, 2003. Rapid determination of REEs and other trace elements in geological samples by microwave digestion and ICP-MS. *At. Spectrosc.* 24 (6), 206–212.
- Basu, A.R., Renne, P.R., Dasgupta, D.K., Teichman, F., Poreda, R.J., 1993. Early and late igneous pulses and a high-³He plume origin for the Deccan flood basalts. *Science* 261, 902–906.
- Beane, J.E., Turner, C.A., Hooper, P.R., Subbarao, K.V., Walsh, J.N., 1986. Stratigraphy, composition and form of the Deccan basalts, Western Ghats, India. *Bull. Volcanol.* 48, 61–83.
- Biswas, S.K., 1980. Structure of the Kutch-Kathiawar region, western India. *Proc. 3rd Indian Geological Congress, Poona*, pp. 255–272.
- Biswas, S.K., 1987. Regional tectonic framework, structure and evolution of the western marginal basins of India. *Tectonophysics* 135, 307–327.

- 826 Biswas, S.K., 2002. Structure and tectonics of Kutch Basin, Western
827 India with special reference to earthquakes. 8th IGC Foundation
828 Lecture, Indian geological Congress, Roorkee, India.
- 829 Biswas, S.K., 2005. A review of structure and tectonics of Kutch
830 basin, western India, with special reference to earthquakes. *Curr.*
831 *Sci.* 88 (10), 1592–1600.
- 832 Biswas, S.K., Deshpande, S.V., 1973. A note on the mode of the
833 eruption of the Deccan trap lavas with special reference to Kutch.
834 *J. Geol. Soc. India* 14 (2), 134–141.
- 835 Bose, M.K., 1973. Petrology and geochemistry of the igneous complex
836 of Mount Girnar, India. *Contrib. Mineral. Petrol.* 39, 247–266.
- 837 Bose, M.K., 1980. Alkaline magmatism in the Deccan province.
838 *J. Geol. Soc. India* 21, 317–329.
- 839 Campbell, I.H., Griffiths, R.W., 1990. Plume-generated triple junctions:
840 key indicators in applying plate tectonics to old rocks.
841 *J. Geol.* 81, 03–433.
- 842 Chatterjee, V.P., Gupta, A.K., Yagi, K., 1992. Geochemical evolution
843 of carbonatite-alkaline complex of Ambadongar, Gujarat, India.
844 Proceedings of the Second Indo-Soviet workshop on experimental
845 mineralogy and petrology, Chemkent, USSR, pp. 139–164.
- 846 Cox, K.G., Hawkesworth, C.J., 1985. Geochemical stratigraphy of the
847 Deccan Traps at Mahabaleshwar, Western Ghats, India, with
848 implications for open system magmatic processes. *J. Petrol.* 26,
849 355–387.
- 850 Das, B., Paul, D.K., Chaudhary, A.K., Ray, A., Patil, S.K., Biswas,
851 S.K., in press. Petrology and geochemistry of Basanitic dykes
852 and Gabbro from northern Kutch, western India: implications on
853 source rock characteristics. *J. Geol. Soc. India.*
- 854 De, A., 1964. Iron-titanium oxides and silicate minerals of the alkali
855 olivine basalts, tholeiites and acidic rocks of the Deccan Trap series
856 and their significance. International Geological Congress Report,
857 22nd session, pt III., vol. 1, pp. 126–138.
- 858 Dessai, A.G., Rock, N.M.S., Griffin, B.J., Gupta, D., 1990. Mineralogy
859 and petrology of some xenolith bearing alkaline dykes associated
860 with Deccan magmatism, south of Bombay, India. *Eur. J. Mineral.*
861 2, 667–685.
- 862 Devey, C.W., Stephens, W.E., 1991. Tholeiite dykes in the Seychelles
863 and the original spatial extent of the Deccan. *J. Geol. Soc. London*
864 148, 979–983.
- 865 Dèzes, P., Schmid, S.M., Ziegler, P.A., 2004. Evolution of the
866 European Rift System: interaction of the Alpine and Pyrenean
867 orogens and their foreland lithosphere. *Tectonophysics* 389, 1–33.
- 868 Downes, H., MacDonald, R., Upton, B.G.J., Cox, K.G., Bodonier, J.-L.,
869 Mason, P.R.D., James, J., Hill, P.G., Heam, B.C., 2004. Ultramafic
870 xenoliths from the Bearpaw Mountain, Montana, USA: evidence for
871 multiple metasomatic events in the lithospheric mantle beneath the
872 Wyoming Craton. *J. Petrol.* 45 (8), 1631–1662.
- 873 Draper, D.S., 1992. Spinel lherzolite xenolith from Lorena Butte
874 Simoco Mountain, southern Washington (USA). *J. Geol.* 100,
875 766–776.
- 876 Duncan, R.A., 1978. Geochronology of basalts from the Ninetyeast
877 ridge and continental dispersion in the eastern Indian Ocean.
878 *J. Volcanol. Geotherm. Res.* 4, 283–305.
- 879 Edgar, A.D., Lloyd, F.E., Forsyth, D.M., Barnett, R.L., 1989. Origin of
880 glasses in upper mantle xenoliths from Quaternary volcanics of Gees,
881 West Eifel, Germany. *Contrib. Mineral. Petrol.* 103, 277–286.
- 882 Erlank, A.J., Waters, F.G., Hawkesworth, C.J., Haggerty, S.E.,
883 Allsopp, H.L., Rickard, R.S., Menzies, M.A., 1987. Evidence for
884 mantle metasomatism in peridotite nodules from the Bultfontein
885 Floors, Kimberley, South Africa. In: Menzies, M.A., Hawkes-
886 worth, C.J. (Eds.), *Mantle Metasomatism*. Academic Press,
887 London, pp. 313–361.
- 888 Evensen, N.M., Hamilton, P.J., O'niions, R.K., 1978. Rare earth
889 abundances in chondritic meteorites. *Geochim. Cosmochim. Acta*
890 42, 1199–1212.
- 891 Fisher, R.A., 1953. Dispersion on a sphere. *Proc. R. Astro. Soc., A.*
892 217, 295–305.
- 893 Francis, D., Ludden, J., 1990. The mantle source for olivine
894 nephelinite, basanite and alkaline olivine basalt at Fort Selkirk,
895 Yukon, Canada. *J. Petrol.* 31 (2), 371–400.
- 896 Govindaraju, K., 1994. A compilation of working values and sample
897 description of 383 Geostandards. *Geostand. Newsl.* 18, 1–158.
- 898 Guha, D., Das, S., Srikarni, C., Chakraborty, S.K., 2005. Alkali Basalt
899 of Kachchh: its implication in the tectonic framework of Mesozoic
900 of western India. *J. Geol. Soc. India* 66, 599–608.
- 901 Karmalkar, N.R., Rege, S., 2002. Cryptic metasomatism in the upper
902 mantle beneath Kutch: evidence from spinel lherzolite xenoliths.
903 *Curr. Sci.* 82 (9), 1157–1165.
- 904 Karmalkar, N.R., Sarma, P., 2003. Characterisation and origin of silicic
905 and alkali rich glasses in the upper mantle-derived spinel peridotite
906 xenoliths from alkali basalts, Deccan trap, Kutch, northwest India.
907 *Curr. Sci.* 85, 386–392.
- 908 Karmalkar, N.R., Rege, S., Griffin, W.L., O'Reilly, S.Y., 2005. Alkaline
909 magmatism from Kutch, NW India: implications for
910 plume-lithosphere interaction. *Lithos* 81, 101–119.
- 911 Kerr, A.C., 2003. Oceanic Plateaus. *Treatise Geochem.* 3, 537–565.
- 912 Krishnamurthy, P., Cox, K.G., 1977. Picrite basalts and related rocks
913 from the Deccan Traps of Western India. *Contrib. Mineral. Petrol.*
914 62, 53–75.
- 915 Krishnamurthy, P., Pande, K., Gopalan, K., Macdougall, J.D., 1989. Upper
916 mantle xenoliths in alkali basalts related to Deccan Trap
917 Volcanism. *Geol. Soc. India, Spec. Publ.*, vol. 10, pp. 53–68.
- 918 Larsen, L.M., Pedersen, A.K., Sundvoll, B., Frei, R., 2003. Alkali
919 picrites formed by melting of old metasomatized lithospheric
920 mantle: Maniitlat Member, Vaigat Formation, Palaeocene, West
921 Greenland. *J. Petrol.* 44 (1), 3–38.
- 922 Le Bas, M.J., 1987. Nephelinites and carbonatites. In: Fitton, J.G.,
923 Upton, B.G.J. (Eds.), *Alkaline Igneous Rocks*. *Geol. Soc. Spec.*
924 *Publ.*, vol. 30, pp. 53–84.
- 925 Le Bas, M.J., Streckeisen, A.L., 1991. The IUGS systematics of
926 igneous rocks. *J. Geol. Soc. London* 148, 825–833.
- 927 Lee, D.-C., Halliday, A.N., Davoies, G.R., Essene, E.J., Fitton, G.,
928 Temdjim, R., 1996. Melt enrichment of shallow depleted mantle: a
929 detailed petrological, trace element and isotopic study of mantle-
930 derived xenoliths and megacrysts from the Cameroon line. *J. Petrol.*
931 37, 415–441.
- 932 Lightfoot, P.C., Hawkesworth, C.J., 1988. Origin of Deccan Trap
933 lavas: evidence from combined trace element and Sr-, Nd- and Pb-
934 isotope studies. *Earth Planet. Sci. Lett.* 91, 89–104.
- 935 Lightfoot, P.C., Hawkesworth, C.J., Devey, C.W., Rogers, N.W., Van
936 Calsteren, P.W.C., 1990. Source and differentiation of Deccan Trap
937 lavas: implication of geochemical and mineral chemical variations.
938 *J. Petrol.* 31, 1165–1200.
- 939 Mahoney, J.J., 1988. Deccan Traps. In: Macdougall, J.D. (Ed.),
940 *Continental Flood basalts*. Kluwer Dordrecht, pp. 141–194.
- 941 Mahoney, J.J., Sheth, H.C., Chandrasekharam, D., Peng, Z.X., 2000. Geochemistry of flood basalts of the Toranmal section, Northern Deccan traps, India: implications for regional Deccan stratigraphy. *J. Petrol.* 41 (7), 1099–1120.
- 942 Maitra, M., 2003. Petrology of the alkaline plugs in Pachcham Island, Kachch District, Gujarat. *Indian J. Geol.* 75 (1-4), 167–190.
- 943 Melluso, L., Beccaluva, L., Brotzu, P., Gregnanin, A., Gupta, A.K.,
944 Morbidelli, L., Traversa, G., 1995. Constraints on the Mantle
945 sources of the Deccan Traps from the Petrology and Geochemistry 949

- 950 of the Basalts of Gujarat State (Western India). *J. Petrol.* 36 (5),
951 1393–1432.
- 952 Melluso, L., Sethna, S.F., Morra, V., Khateeb, A., Javery, P., 1999.
953 Petrology of the Mafic dykes Swarm of the Tapi River in the
954 Nandurbar area (Deccan Volcanic Province). *Mem. - Geol. Soc.*
955 *India* 43, 735–756.
- 956 Melluso, L., Mahoney, J.J., Dallai, L., 2006. Mantle sources and
957 crustal input as recorded in high-Mg Deccan Traps of basalts of
958 Gujarat (India). *Lithos* 89, 259–274.
- 959 Mukherjee, A.B., Biswas, S., 1988. Mantle derived spinel lherzolite
960 xenoliths from the Deccan Volcanic Province (India): implication
961 for the thermal structure of the lithosphere underlying the Deccan
962 Traps. *J. Volcanol. Geotherm. Res.* 35, 269–276.
- 963 Pande, K., Venkatesan, T.R., Gopalan, K., Krishnamurthy, P.,
964 Macdougall, J.D., 1988. ^{40}Ar – ^{39}Ar Ages of alkali basalts from
965 Kutch, Deccan Volcanic Province, India. *Mem. - Geol. Soc. India*
966 10, 145–150.
- 967 Paul, D.K., Potts, P.J., Rex, D.C., Beckinsale, R.D., 1977. Geochem-
968 ical and petrogenetic study of the Gimar igneous complex, Deccan
969 volcanic province. *Bull. Geol. Soc. Am.* 88, 227–234.
- 970 Pearce, J.A., 1983. Role of the subcontinental lithosphere in magma
971 genesis at active continental margins. In: Hawkesworth, C.J.,
972 Norry, M.J. (Eds.), *Continental Basalts and Mantle Xenoliths*.
973 Shiva, Orpington, pp. 230–249.
- 974 Pilet, S., 2001. The origin of Cantal alkali basalts (Massif Central,
975 France): Mineralogical and Geochemical constraints for a
976 heterogeneous mantle source. Unpub. PhD Thesis, University de
977 Lausanne.
- 978 Raval, U., 2001. Earthquakes over Kutch: a region of ‘Trident’ Space–
979 Time Geodynamics. *Curr. Sci.* 81, 809–815.
- 980 Ray, A., Patil, S.K., Paul, D.K., Biswas, S.K., Das, B., Pant, N.C.,
981 2006. Petrology, geochemistry and magnetic properties of Sadara
982 sill: evidence of rift-related magmatism from Kutch basin,
983 northwest India. *J. Asian Earth Sci.* 27, 907–921.
- 984 Richards, M.A., Duncan, R.A., Courtillot, V.E., 1989. Flood basalts
985 and hotspot tracks: plume heads and tails. *Science* 246, 103–107.
- 1019
- Rock, N.M.S., Griffin, B.J., Edgar, A.D., Paul, D.K., Hergt, J.M., 986
1992. A spectrum of potentially diamondiferous lamproites and 987
minettes from the Jharia coalfield, eastern India. *J. Volcanol.* 988
Geotherm. Res. 50, 55–83. 989
- Sen, G., Cohen, T.H., 1994. Deccan intrusion, crustal extension, 990
doming and the size of the Deccan-Reunion plume head. In: 991
Subbarao, K.V. (Ed.), *Volcanism*. Wiley Eastern, pp. 201–216. 992
- Sheth, H.C., Chandrasekharan, D., 1997. Plume-rift interaction in the 993
Deccan volcanic province. *Phys. Earth Planet. Inter.* 99, 179–187. 994
- Shukla, A.D., Bhandari, N., Kusumgar, S., Shukla, P.N., Ghevariya, Z.G., 995
Gopalan, K., Balaram, V., 2001. Geochemistry and magnetostrati- 996
graphy of Deccan flows at Anjar, Kutch. *Proc. Indian Acad. Sci.*, 997
A Earth Planet. Sci. 110, 111–132. 998
- Simonetti, A., Goldstein, S.L., Schmidbeger, S.S., Viladkar, S.G., 999
1998. Geochemical and Nd, Pb and Sr isotopic data from Deccan 1000
Alkaline Complexes — inferences for mantle sources and Plume- 1001
Lithosphere interaction. *J. Petrol.* 39, 1847–1864. 1002
- Sun, S.S., McDonough, W.F., 1989. Chemical and isotope systematics 1003
of oceanic basalt: implication for mantle composition and 1004
processes. In: Saunders, A.D., Norry, M.J. (Eds.), *Magmatism* 1005
in the Ocean Basins. *Geol. Soc. London. Spec. Publ.*, vol. 42. 1006
Blackwell Scientific Publisher, pp. 313–345. 1007
- Vandamme, D., Courtillot, V., 1992. Paleomagnetic constraints on the 1008
structure of the Deccan traps. *Phys. Earth Planet. Inter.* 74, 241–261. 1009
- Vandamme, D., Courtillot, V., Besse, J., 1991. Paleomagnetism and age 1010
determinations of the Deccan Traps (India): results of a Nagpur– 1011
Bombay traverse and review of earlier work. *Rev. Geophys.* 29, 1012
150–190. 1013
- Wilson, M., 1989. *Igneous Petrogenesis: A global tectonic approach.* 1014
Unwin Hyman, London. 1015
- Yaxley, G.M., Kamensky, V., Green, D.H., Falloon, T.J., 1997. Glasses 1016
in mantle xenoliths from western Australia and their relevance to 1017
mantle processes. *Earth Planet. Sci. Lett.* 148, 433–446. 1018